Earth-Science Reviews 226 (2022) 103957

Contents lists available at ScienceDirect

Earth-Science Reviews

journal homepage: www.elsevier.com/locate/earscirev

Recent climate and hydrological changes in a mountain–basin system in Xinjiang, China

Junqiang Yao [a,*], Yaning Chen [b,*], Xuefeng Guan [c], Yong Zhao [d], Jing Chen [a], Weiyi Mao [a]

[a] Institute of Desert Meteorology, China Meteorological Administration, Urumqi 830002, China
[b] State Key Laboratory of Desert and Oasis Ecology, Xinjiang Institute of Ecology and Geography, Chinese Academy of Sciences, Urumqi, China
[c] Geography Department, Humboldt-Universität zu Berlin, Germany
[d] School of Atmospheric Science, Chengdu University of Information Technology, Chengdu, China

ARTICLE INFO

Keyword:
Mountain–basin system
Climate warming
Hydrologic effect
Arid regions
Endorheic basins
Xinjiang

ABSTRACT

Xinjiang, China, is a representative arid region in Central Asia that is characterized by a unique mountain–basin structure and fragile mountain–oasis–desert ecosystems. Climate warming directly affects hydrological changes and may threaten water availability and ecological security in Xinjiang (XJ). In this study, we conducted a systematic review of recent climatic changes and their effects on hydrological system changes in XJ. The XJ climate has experienced significant warming and moistening during 1961–2018, and the most dramatic increase has occurred since the mid-1980s. Climate extremes have become increasingly notable in the warming climate, resulting in increases in precipitation and warm extremes and decreases in cold extremes. Moreover, accelerated local precipitation recycling has been triggered by an increasingly warm–wet climate and enhanced evaporation. The accelerated climate warming in XJ has caused significant glacier shrinkage, decreased snow cover and snowfall fraction, aggravated meteorological drought, increased river runoff, and lake expansion. The climate-related changes in the hydrological regimes may have adverse ecological effects, including increased soil moisture loss, reduced growing season vegetation growth, and shrinkage of the desert–oasis ecotone. Despite many achievements in climate and hydrological change research in XJ, we suggest that there is an urgent need to improve the comprehensive ground observation network, reproduce climate variability findings using multiple datasets, reveal the underlying physical mechanisms, and assess the hydro-meteorological disaster risks of a warming climate in the future. In addition, a conceptual framework of the climate and hydrological changes in mountain–basin system proposed, which is expected to contribute to the understanding of arid region hydrology in the future.

1. Introduction

Because of low precipitation, high temperatures, sparse vegetation coverage, and fragile ecosystems, arid lands are among the fastest warming and most sensitive regions to climate change, exhibiting accelerated expansion under such conditions (IPCC, 2013; Huang et al., 2016a, 2016b, 2017b). Central Asia is one of the driest regions and the largest non-zonally arid area worldwide. The arid Xinjiang region of China is a representative arid region of Central Asia (Josef et al., 1997; Li et al., 2017a; Yao et al., 2020a). The XJ is in the core region of Asian westerlies (westerly-dominated climate regime) (Huang et al., 2015; Chen et al., 2009) and the upstream area of East Asian climate conditions. Its climate is primarily controlled by the intensity and location of the westerly circulation and varies significantly from the subtropical arid and monsoonal regions (Aizen et al., 2001; Huang et al., 2013). Notably, the region is characterized by a unique mountain–basin structure and fragile mountain–oasis–desert ecosystems (Chen et al., 2019a, 2019b; Yao et al., 2020a). In addition, this region is a core region of the "Silk Road Economic Belt" and is crucial for the future sustainable development of China (Chen et al., 2020).

The mountain–basin system in XJ is a unique representation in Central Asia and the world (Fig. 1). It comprises a typical mountain–basin landscape and exhibits distinct hydrological cycle processes consisting of precipitation, glaciers, snowfall, river runoff, and enclosed lakes with ecosystems consisting of mountains, oases, deserts, and desert–oasis ecotone environments. In the arid regions of XJ, the

* Corresponding authors.
E-mail address: yaojq1987@126.com (J. Yao).

https://doi.org/10.1016/j.earscirev.2022.103957
Received 31 December 2020; Received in revised form 6 December 2021; Accepted 31 January 2022
Available online 5 February 2022

mountain and plateau regions are the largest reservoirs of ice and snow in regions with abundant precipitation and supply vital water to many large rivers and lakes (Chen et al., 2019a, 2019b, Chen et al., 2020). Mountainous precipitation is the principal source of the water resources of the XJ regions, where is limited to wet season rainfall and winter snow. Changes in precipitation will have critical impacts on water resources and cryosphere and biosphere systems (Yao et al., 2021). Known as the water towers in XJ, the mountain region is particularly crucial for water resources and ecological security, oases sustainability, and Silk Road economic development in the arid regions. The depression basins converge in surface rivers and meltwater from mountains and groundwater from underground aquifers, leading to the formation of oases. The oasis, as an intrazonal ecological landscape situated within desert environments, plays a critical role in sustaining life and yielding benefits to humans, sustaining agricultural production, protecting biodiversity, regulating the local climate, and providing ecosystem services in arid regions (Cheng et al., 2006; Xue et al., 2015, 2019; Zhang et al., 2017a).

Recently, climate change in arid China, especially in XJ, has varied significantly and attracted significant attention (Shi et al., 2003, 2007; Li et al., 2012; Chen et al., 2015; Yao et al., 2018a; Chen et al., 2019a; Wu et al., 2019; Wang et al., 2020a; Yao et al., 2020a, 2020b, 2020c; Chen et al., 2020). The arid region surrounding XJ has significantly warmed and gained moisture according to in situ observations and re-analyses. Shi et al. (2003) reported that the climate in arid China changed from warm–dry to warm–wet in the mid-1980s. The annual warming rate in XJ was found to be 0.34 °C per decade during 1961–2010 (Yao et al., 2020b). Moreover, the climate has become wetter in XJ based on Standardized Precipitation Index (SPI) data (Zhang et al., 2012; Li et al., 2016a), while the climate has experienced a significant wet-to-dry shift in XJ since 1997 (Yao et al., 2018a). Wang et al. (2020b) investigated the warming–wetting trend in XJ from multiple perspectives. Rapid warming and increased precipitation have accelerated the water cycle and have led to changes in the hydrological processes that rely on mountainous precipitation and meltwater from ice and snow in the arid catchments (Chen, 2020; Chen et al., 2015, 2019a; Shen et al., 2020). Recently, significant progress has been made in assessing the changes in hydrological processes and their mechanisms in XJ (Chen et al., 2006, 2007, 2009, Chen et al., 2013b; Sun et al., 2013; Fang et al., 2018; Shen

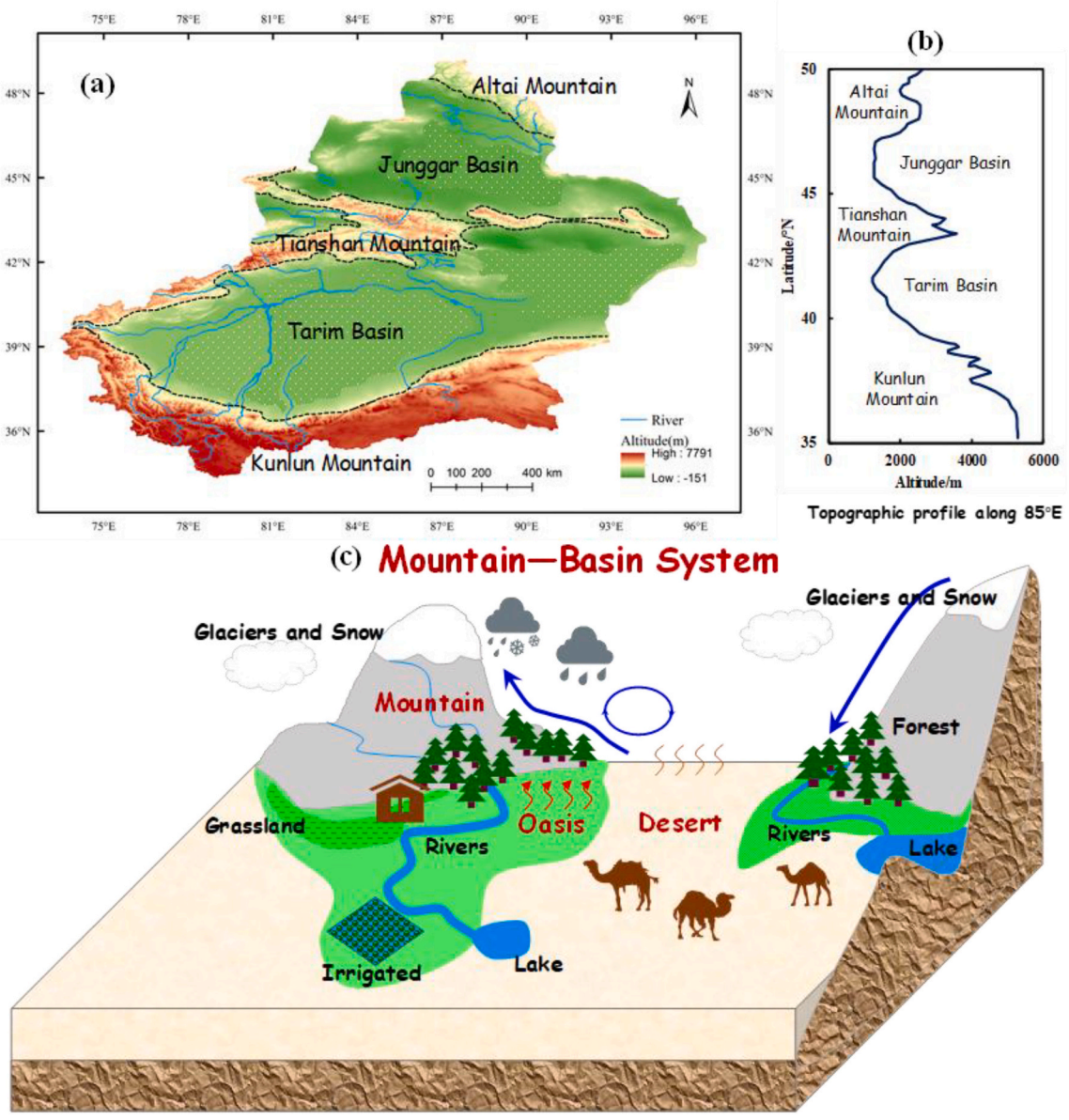

Fig. 1. Topographic map (a) of XJ, including key mountains and basins. (b) Topographic profile along 85°E. (c) Sketch of mountain–basin system and associated hydrological cycle system in XJ.

et al., 2018). However, significant progress has mainly been achieved regarding the basin scale and cannot be generalized to achieve a comprehensively knowledge of climate change effects on hydrological regimes throughout the XJ region.

Although many studies have yielded significant findings regarding climate and hydrological changes in XJ, uncertainties remain. This study aimed to systematically review recent studies and attempt to quantify the recent changes in climate and hydrological systems. The remainder of this paper is organized as follows. Section 2 describes the study region and the data. The climate background and recent climate changes observed in arid XJ are summarized in Section 3. Section 4 explores the hydrological system changes in glaciers, snow, runoff, and lakes. Section 5 proposes several implications of climatic and hydrological changes in the mountain–basin regions, and Section 6 summarizes the state of knowledge on climate and hydrological system changes in arid XJ, China.

2. Study region and data

2.1. Study region

The XJ region (hereafter referred to as XJ) is in northwest China, situated in eastern Central Asia in the Eurasian hinterland, which is characterized by a wide distribution of deserts, oases, glaciers, and snow cover. This region extends from Altai Mountain in the north to Kunlun Mountain in the south and from the Pamir and Western Tianshan Mountains to the Gobi Desert in the east, covering a total area of 1.66×10^6 km^2. As the core region of Central Asia, it is far from any ocean and is one of the most arid regions worldwide (Li et al., 2017b). Tianshan Mountain, the "water tower of Central Asia," spans XJ. The terrain of XJ is characterized by three mountain ranges that surround the two desert basins, resulting in a unique mountain–basin system (Fig. 1) with distinct hydrological processes.

In terms of global warming effects, the mountain–basin system is especially fragile. In XJ, water originates predominantly from mountainous snow, glacial meltwater, and mid-mountainous precipitation (Chen et al., 2015), which feed numerous inland rivers. The basin primarily spans the vast Gobi Desert with few oases. It has a desert climate with an annual total precipitation of less than 50 mm. The oasis economy and desert ecology in XJ have become more acute because of the overuse of water resources. The hydrological processes in the XJ region are sensitive to global warming, including decreasing glacier and snow cover, changing runoff, and expanding lakes.

2.2. Data

2.2.1. Meteorological data

The observed daily mean temperature, maximum and minimum temperatures, and precipitation data were provided by the National Meteorological Information Center, China Meteorological Administration (CMA) (http://www.nmic.gov.cn/). Modern meteorological observation stations in XJ began operations in 1951. To guarantee consistency, the daily records were of sufficient quality, exhibiting a relatively homogenous spatial distribution, and have been recorded since before 1961. As a result, 89 of 105 stations were selected to obtain daily data from January 1, 1961, to December 31, 2018. In addition, the extreme climate indices for the warm days (TX90p), warm nights (TN90p), cold days (TX10p), cold nights (TN10p), Max Tmax (TXx), Min Tmin (TNn), number of torrential rainfall days (R24, the torrential rainfall was defined as the precipitation of 24 h exceeded 24 mm in XJ, Yao et al., 2018b), and maximum 1-day precipitation amount (RX1day) were calculated using the RclimDex procedure (Zhang et al., 2011). Potential evaporation (PET) was estimated using the Penman–Monteith (P-M) equation, and the actual evapotranspiration (AE) was estimated using the Budyko theory (Fu, 1981; Yao et al., 2020a). We used an analytical solution of the Budyko theory was proposed by Fu (1981) and can be expressed as:

$$\frac{ET}{P} = 1 + \frac{PET}{P} - \left[1 + \left(\frac{PET}{P}\right)^{\overline{w}}\right]^{1/\overline{w}} \quad (1)$$

where $\overline{w}$ is a parameter dominated by the water-energy partitioning and related to the land surface conditions (Yang et al., 2006; Li et al., 2013a; Li et al., 2013b). Yao et al. (2017) developed an empirical and physically-based model to parameterize $\overline{w}$ for inland arid regions, and can be written as:

$$\overline{w} = 1 + 81.513\left(\frac{S_{max}}{\overline{PET}}\right)^{1.621}(A)^{-0.0233}exp(-2.218tan\beta) \quad (2)$$

where $\frac{S_{max}}{PET}$ is the relative soil water storage, A is the area of the modeled region, and $tan\beta$ is the slope of the study region.

2.2.2. Glacier data

The glacier area and volume data in China were investigated according to the first glacier inventory (FGI; indicating the glacier status from 1950 to the 1980s) and second glacier inventory (SGI; indicating the glacier status from 2004 to 2010) (Qin et al., 2005; Shangguan et al., 2009; Liu et al., 2015). The glacier mass balance, glacier area and length, and retreating rate of the east and west branches of Urumqi Glacier No. 1 (UG1) were sourced from the Bule Book on Climate Change in China: 2019 (China Meteorological Administration (CAM), 2019). In addition, changes in the glaciers in the XJ were evaluated based on data selected from previous studies.

2.2.3. Runoff data

This study reviewed the changes in runoff for 18 large rivers in XJ and the surrounding area. The runoff data for nine rivers in XJ (i.e., Kaidu, Kunque, Kunmalike, Tuoshigan, Tarim, Kashgar, Yarkant, Karakash, and Yulongkash Rivers) were provided by the XJ Hydrological Bureau for 1957–2017, the data for the other rivers were based on data selected from previous studies.

2.2.4. Lake data

The lake area data for 33 large lakes (>10 km^2) in XJ were sourced from Li et al. (2018) based on Landsat satellite data (TM/ETM+/OL). The Bosten Lake level data from 1961 to 2019 were sourced from the Xinjiang Tarim River Basin Management Bureau in China (http://www.tahe.gov.cn/Category_1/Index.aspx).

2.2.5. Atmospheric moisture budget

The ERA-Interim reanalysis dataset was used to calculate the moisture flux in XJ. We estimated the annual moisture transport entering XJ via the four-boundary moisture budget. The moisture transport properties included the monthly mean specific humidity, meridional and zonal winds, and surface pressure data for 1979–2012. The data had a horizontal resolution of $1^\circ \times 1^\circ$.

3. Climate background and climate change

3.1. Rapid atmosphere warming

The climate in XJ is characterized by high air temperatures, a high diurnal temperature range (DTR), low precipitation and humidity, and high seasonal variations (Yao et al., 2020a). The annual mean air temperature across XJ is approximately 8 °C and decreases from south to north (<4 °C in the northern XJ) (Yao et al., 2020a). XJ has undergone rapid warming in recent decades (Shi et al., 2007; Zhang et al., 2012; Jiang et al., 2013; Wu et al., 2010; Xu et al., 2010, 2015; Li et al., 2011b; Chen et al., 2006, 2007, 2009, 2014, 2015; Yao et al., 2020b; Li et al., 2021). During 1961–2010, the warming rate reached 0.33 °C /decade (Yao et al., 2020b), which is substantially higher than that of China

overall (0.25 °C/decade) (Li et al., 2012) and the global average (0.12 °C/decade for 1951–2012) (IPCC, 2013). However, published records (Kang et al., 2010; Yao et al., 2019a) have suggested that the strongest warming occurred in the Third Pole region. The temperature in XJ during 1960–2006 increased by approximately 1.8 °C, with a warming rate of 0.36 °C/decade (Piao et al., 2010), which reflects the averages for the third pole region during the same period (Wang et al., 2008). A sharp warming occurred in the late 1980s, with an accelerated warming rate (0.48 °C/decade) from 1990 to 2010 compared with the increase for 1961–1989 (0.10 °C/decade) (Yao et al., 2020b). The global surface air temperatures have experienced a warming "hiatus" since 1998 (Kosaka and Xie, 2013; Karl et al., 2015). Similarly, the increasing trend of the mean temperature in XJ has slowed since 1998; however, it has remained the warmest period on record (Chen et al., 2015; Yao et al., 2018a).

Fig. 2 shows the changes in the annual mean temperature averaged over 89 sites in XJ during 1961–2018. A significant warming rate of 0.30 °C/decade ($p < 0.01$) was determined for the annual mean. For the same period, the observed warming trend was 0.24 °C/decade and 0.37 °C/decade in eastern China and the Tibetan Plateau (TP), respectively (China Meteorological Administration (CAM), 2019). The annual mean temperature rate of increase was 0.30 °C/decade in Central Asia from the 1960s to the 2000s (Yu et al., 2020). These results revealed that the XJ warming rate was consistent with that of Central Asia, higher than that of eastern China, and lower than that of the TP region. The strongest warming was observed in the winter temperatures, with a rate of 0.42 °C/decade (Li et al., 2021), which is the largest contributor to the annual mean (Li et al., 2012; Chen et al., 2015). The warming rate decreased from north to south, and the strongest warming occurred in northern XJ and the mountainous regions (Xu et al., 2010; Kong and Pang, 2012; Li et al., 2021; Yao et al., 2020b).

From 1961 to 2018, both the annual mean minimum air temperature (*Tmin*) and maximum air temperature (*Tmax*) in XJ demonstrated significant increasing trends, with rates of 0.44 °C/decade and 0.22 °C/decade, respectively (Fig. 2b-c). The data indicated asymmetric warming trends in XJ, where the *Tmin* rate was twice as high as the *Tmax*

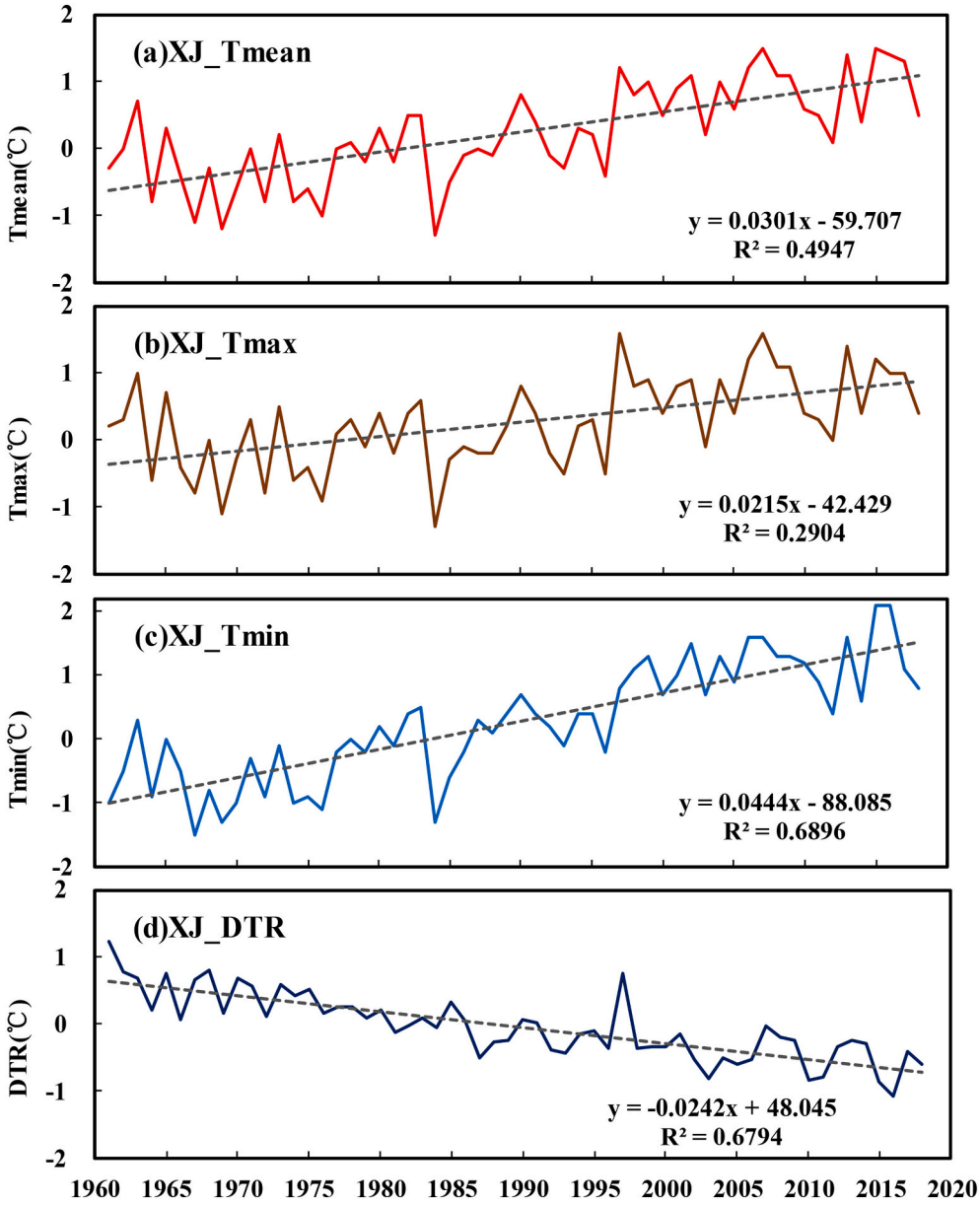

Fig. 2. Time series of annual mean air temperature (Tmean, a) anomalies, maximum (Tmax, b) and minimum (Tmin, c) air temperature anomalies and DTR (d) in XJ. The anomaly was calculated based on 1971–2000 climatological data.

rates. Thus, the DTR decreased significantly by 0.24 °C/decade during 1961–2018 (Fig. 2d). These data demonstrate the accelerated warming in XJ over recent decades.

3.2. Precipitation increases

The average annual precipitation in XJ is below 200 mm (Yao et al., 2020a) and gradually decreases from northwest to southeast from approximately 900 mm (Hao et al., 2018) to less than 30 mm, respectively (Fig. 3a). Most precipitation occurs in summer mouths, accounting for 40%–70% of the annual precipitation (Yao et al., 2020a). Furthermore, the areas with the annual precipitation of >400 mm account for only 12.3% of XJ (Yao et al., 2020b), which is primarily distributed according to elevation height (Fig. 3b). Generally, the

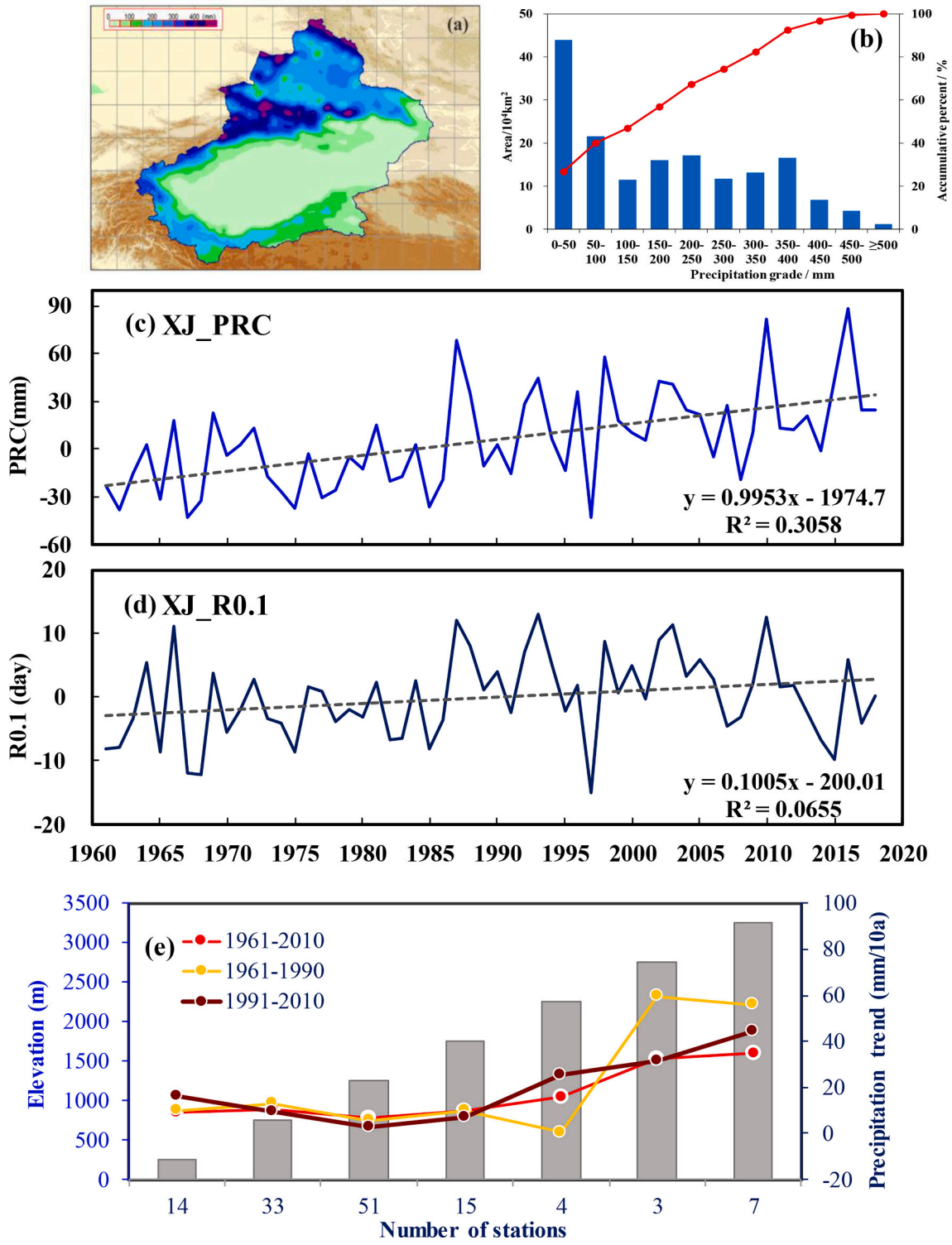

Fig. 3. (a) Climatological precipitation distribution and (b) proportion of area with different precipitation grades in XJ (modified from Yao et al., 2020b). Time series of annual mean precipitation (c) and number of precipitation days (d) during 1961–2018. The anomaly was calculated using 1971–2000 climatological data. (e) Elevation dependence of annual mean precipitation trends for 1961–2010 (modified from Yao et al., 2016b).

precipitation distributions are consistent with the elevation pattern due to orographic effects, based on observations and multiple datasets (Yao et al., 2016a, 2020c).

The annual precipitation in XJ has exhibited a significant increasing trend (7.40 mm/decade for 1961–2008 or 9.46 mm/decade during 1961–2010) (Zhang et al., 2012; Yao et al., 2020b), with a sharp increase in 1987 (Shi et al., 2007; Chen et al., 2015). More dramatically, the rate of increase in the precipitation decreased in the 1990s (Chen et al., 2015), even though precipitation decreased slightly during 1997–2015 (−0.679 mm/decade) (Yao et al., 2018c). The TP precipitation has also demonstrated fluctuations without a clear trend after 1990 (Li et al., 2019). During the period from 1961 to 2018, the annual precipitation significantly increased, with a rate of 9.95 mm/decade (Fig. 3c). The increase in precipitation decreased from northwest to southeast, and the largest increase was observed in the Tianshan Mountains, followed by the northern and southern parts of XJ (Fig. 4; Shi et al., 2007; Xu et al., 2010; Zhang et al., 2010; Shen et al., 2020; Yao et al., 2020b). Seasonally, summer precipitation has contributed strongly to annual precipitation increases in XJ (Li et al., 2011b; Chen et al., 2013a; Yao et al., 2020b). However, summer and winter precipitation contributed equally to the annual precipitation increases in the northern XJ. Additionally, the number of precipitation days (R0.1, total annual number of days with precipitation $\geq$ 0.1 mm/day) slightly increased by 1.0 days/decade during 1961–2018 (Fig. 3d). The R0.1 decreased slightly since the mid-1990s owing to the increase in extreme precipitation days.

Many published records have suggested an elevation-dependent warming (EDW) phenomena in mountain regions globally, based on multi-source data and climate models (Pepin et al., 2015). However, EDW has not been systematically analyzed in XJ. Li et al. (2011b) suggested a warming trend independent of the elevation in XJ. In contrast, Gao et al. (2020) identified significant EDW signals in the Tianshan Mountains from a multi-scale perspective, based on a unique high-resolution dataset. The elevation dependence of the precipitation trends is more complex. Shen et al. (2020) found that precipitation trends were not homogeneous in the Tianshan Mountains and exhibited a rapid increase below 2,000 m in the northern and western Tianshan Mountains (Aizen et al., 1997). However, Yao et al. (2016a) proposed elevation-dependent wetting (EDWE) in the arid regions of China, including XJ (Fig. 3e). The summer TP also exhibited an EDWE phenomena (Li et al., 2017a). However, detecting the EDW and EDWE phenomena is challenging in complex mountainous terrain owing to the scarcity of observed data.

Due to the complex topography and changing climate in XJ, where observational data are scarce, one of the main challenges in studying precipitation and hydrological changes is the uncertainty of data. Yao et al. (2020c) evaluated the eight gridded precipitation datasets and found that the multiple datasets reasonably capture the climatology, seasonality, interannual variability, and spatiotemporal patterns of XJ precipitation, but there are discrepancies of the long-term trends. High-resolution satellite precipitation datasets can help to monitor precipitation changes over ungauged areas (Zhang et al., 2017d). Gao et al. (2018) evaluated the high-resolution satellite precipitation datasets, and suggested that the CHIRPS (Climate Hazards Group Infrared Precipitation with Stations data) is more accurate in reflecting the spatial distribution of average monthly and annual precipitation in XJ. Zhang et al. (2017d) proposed a new statistical downscaling algorithm based on the relation between the Tropical Rainfall Measuring Mission (TRMM) 3B43 precipitation and NDVI, and found that the downscaled TRMM precipitation was accurate in describing the spatial patterns of precipitation in XJ.

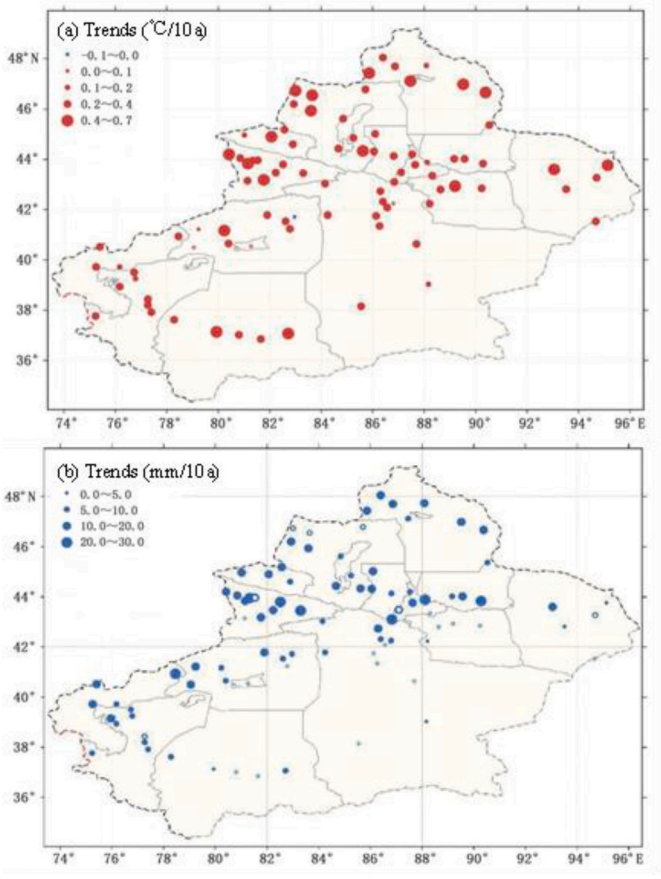

Fig. 4. Spatial changes in the change trends for annual mean air temperature (a) and annual mean precipitation (b) in XJ (modified from Zhang et al., 2021).

3.3. Intensification of extreme climate

Climate extremes are closely correlated with current climate changes and are major contributors to climate and hydrological dynamics. The observed records indicate that the magnitude and frequency of extreme climate events have increased in the XJ during recent decades (Chen et al., 2014; Deng et al., 2014; Wang et al., 2017; Yao et al., 2018b). Climate warming has resulted in increases in warm extremes and decreases in cold extremes. The TX90p and TN90p increased by 3.6 d/decade and 6.9 d/decade, while the TX10p and TN10p decreased by 2.9 d/decade and 8.0 d/decade during 1961–2018, respectively (Fig. 5). These data indicate that the magnitudes of the cold and warm nights were greater than those for cold and warm days. The precipitation-related extremes demonstrated an increasing trend in XJ; the R24 increased by 0.96 d/decade, and the RX1day increased by 0.86 mm/day/decade during 1961–2018 (Fig. 5). The extreme precipitation tends to occur more severely and frequently after the 1980s (Yao et al., 2020a). In particular, the extreme precipitation exhibited strong interannual variations since the 21st century, with greater uncertainties. spatially, the extreme precipitation trends showed a heterogeneity in XJ (1961-2018), and the significant increasing trend was concentrated in the Tianshan Mountains and in northern XJ (Hu et al., 2021). Thus, the risk of floods in XJ is expected to increase, especially in the Tianshan Mountains.

3.4. Enhanced evapotranspiration

Evaporation is a key element of the hydrological cycle and energy balance, and it reflects the transformation of water from the liquid to the gaseous state (Li et al., 2019). Many studies have indicated that PET has exhibited a decreasing trend worldwide, especially in the Northern Hemisphere (Brutsaert and Parlange, 1998; Roderick and Farquhar, 2002; Roderick et al., 2007; Cong et al., 2009; Yang and Yang, 2011). There is controversy regarding the decreasing PET associated with rising

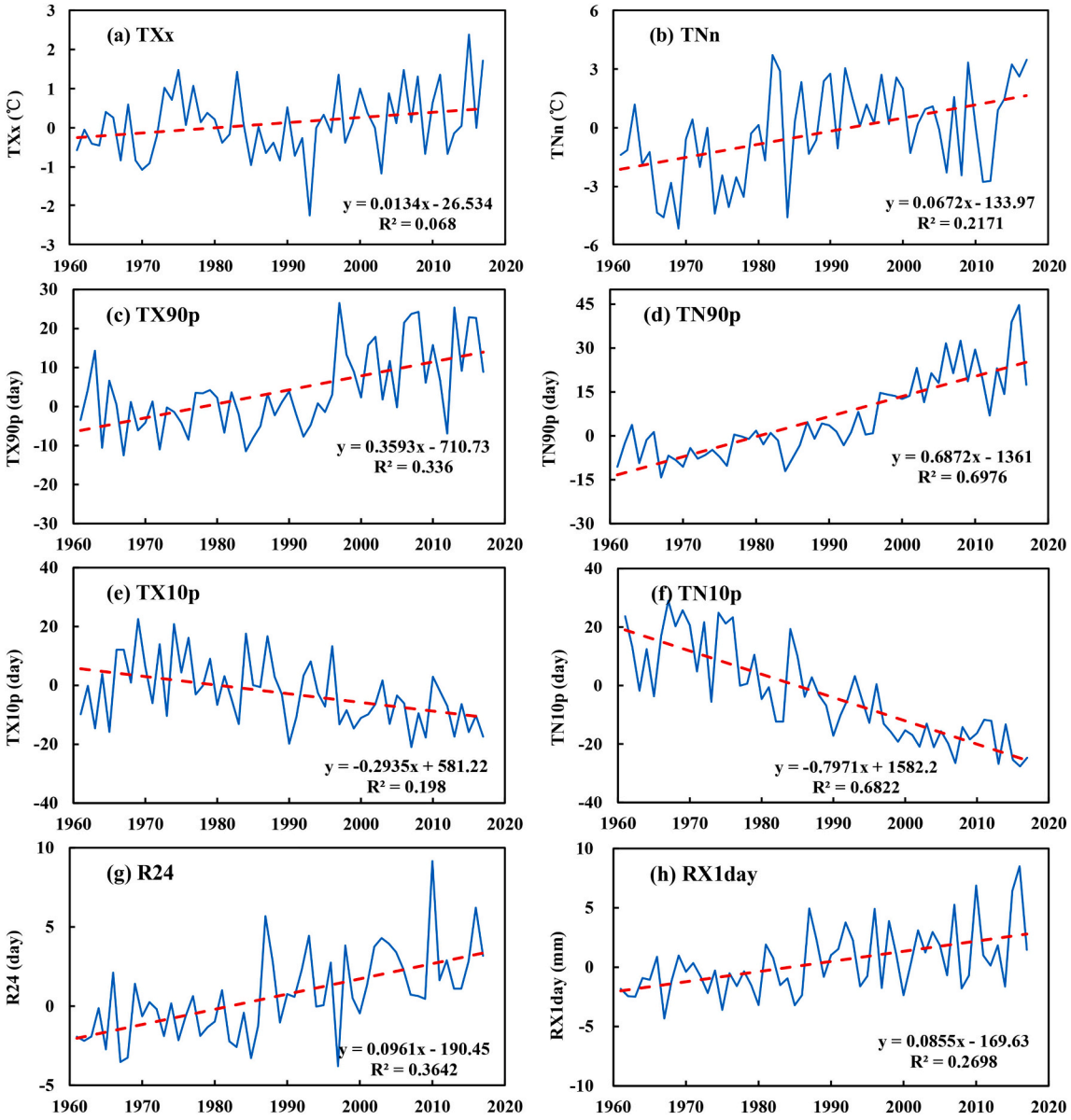

Fig. 5. Temporal variations in the extreme climate index for 1961–2018 in XJ. The anomaly was calculated based on the 1971–2000 climatological data.

temperatures, widely termed as the "evaporation paradox" (Roderick and Farquhar, 2002). Li et al. (2013b) proposed a new explanation for the pan evaporation dynamics in arid China based on a PenPan model, in which pan evaporation exhibited a significant downward trend during 1958–1993 (60 mm/decade) and then has increased since 1993 (107 mm/decade). This is consistent with the calculated PET (Fig. 6a).

AE is difficult to observe directly on a large scale (Gao et al., 2012). Thus, it is typically estimated using remote sensing and models. The AE estimated by the Budyko model in XJ was consistent with the water balance result from the 56 basins and MODIS ET product for this study area (Yao et al., 2017, 2020b). The estimated AE increased by 6.66 mm/decade in XJ from 1961 to 2010 (Fig. 6b). Based on the MODIS data, the regional average annual AE in XJ was 365.7 mm during 2003–2013 (Yao et al., 2019b), and higher values were observed in the Tianshan Mountains, Yili River valley, and Altai Mountains (Fig. 6c). In addition, there was a significant increasing trend in the northern slopes of the Tianshan Mountains and along the Tarim River Basin, which is distributed across irrigated districts and riverways. However, the decreasing trend occurred predominantly in the mountainous region, which is comprised of mostly natural vegetation cover (Fig. 6d). This indicates an accelerated water transformation from liquid to gaseous states in XJ due to climate warming, particularly in oasis-irrigated regions.

3.5. *Projected future climate change*

Although the projections of changes in mean and extreme temperature and precipitation present greater uncertainties (Piao et al., 2010; Guo et al., 2017), these are expected to increase in the future in XJ (Shi et al., 2007; Wang et al., 2017; Wang et al., 2021). In particular, model projections have suggested a warmer and wetter tendency on the XJ in the 21-st century compared with other regions in China (Wang and Chen, 2014; Zhou et al., 2014). The regional mean increases in annual air temperature are as 3 °C and 1–2 °C in the northern and southern XJ, respectively, during 2046–2075 (relative to 1971–2100) under representative concentration pathway (RCPs) (Guo and Shen, 2016). Precipitation was expected to increase by 5–10%, and to increase more significantly in mountainous regions in the future (Wang and Chen, 2014; Guo and Shen, 2016). In addition, temperature is projected to increase robustly while precipitation should experience a slightly increase in the basin areas (Chen et al., 2013b; Xu et al., 2016). Despite the

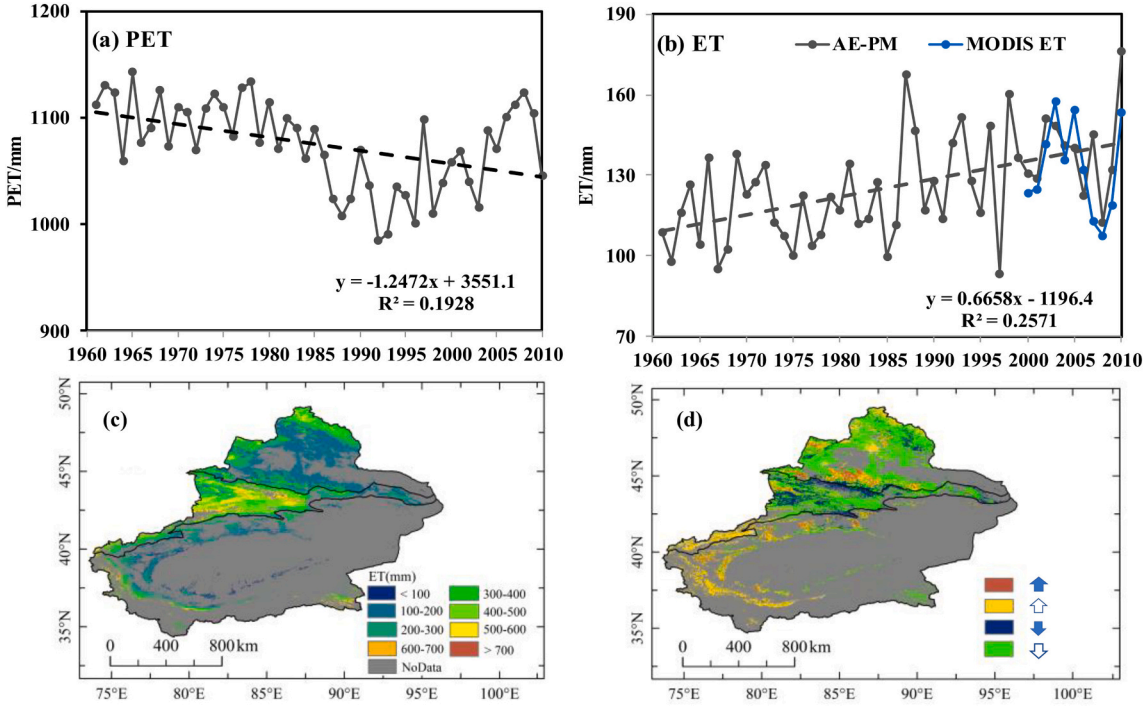

Fig. 6. Temporal variations in the annual PET (a) and AE (b) in XJ (modified from Yao et al., 2020c; blue line represents the MODIS ET). Spatial distribution (c) and rate of change (d) in the annual mean ET in XJ during 2003–2013 (modified from Yao et al., 2019b).

uncertainties, the duration of warm extremes (TN90p and TX90p) was projected to become longer in southern XJ and the frequency of cold extremes (TN10p and TX10p) are predicted to decrease in Tianshan Mountain, and the frequency of precipitation extremes events are expected to increase in Tianshan Mountain based on the CMIP6 model simulations under the two scenarios (2015-2100, SSP245 and SSP585) (Guan et al., 2021).

4. Hydrological change in mountain–basin system

Climate warming has directly affected the hydrological system in XJ, leading to glacier retreat, decreasing snow cover and snowfall fractions, and increasing river runoff and lake expansion.

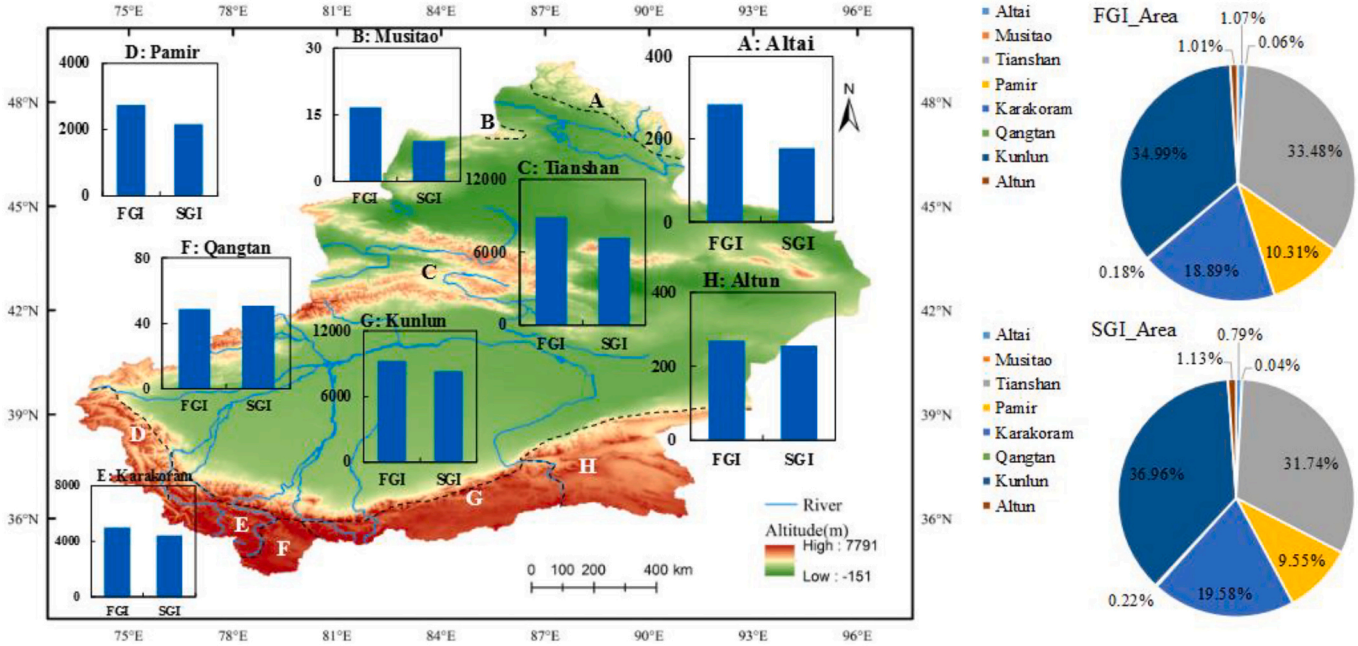

Fig. 7. (Left) Spatial distribution of glacier area changes between the FGI to SGI in XJ (x-axis is the glacier inventory and y-axis is the glacier area, unit: km^2). (**Right**) Proportion of the glacier area in the sub-regions in XJ in the FGI and SGI. **A**: Altai Mountains. **B**: Musitao Mountains. **C**: Tianshan Mountains. **D**: Pamir Plateau. **E**: Karakoram. **F**: Qangtang Plateau. **G**: Kunlun Mountains. **H:** Altun Mountain.

4.1. Glacier shrinkage

Glaciers are a sensitive indicator of climate variability and have been shrinking worldwide owing to global warming (Roe et al., 2017). According to the FGI, XJ contains 20,319 glaciers with an area of 26,537.8 km^2 and an approximate volume of 2,517.5 km^3 (Qin et al., 2005; Shangguan et al., 2009; Fig. 7; Fig. 8). The SGI identified 20,695 glaciers with a total area of 22,623.8 km^2 and a volume of 2,155.8 km^3 (Liu et al., 2015; Fig. 7; Fig. 8). Approximately 88% of the total glaciers, glacier area, and ice reserves were concentrated in the Tianshan, Kunlun, and Kala Kunlun Mountains. Changes in the glacial area and ice volume measured in XJ and its sub-regions are presented in Figures 7 (Fig. 8) for the FGI (SGI) periods. The glacial area and ice volume in XJ decreased by 14.7% and 14.4%, respectively, between the FGI and SGI periods. Among the mountain ranges, the Musitao Mountains (region B) exhibited the largest glacier retreat rate; the change in glacial area and ice volume decreased by 46.2% and 49.4% between the FGI to SGI periods, respectively. For the Altai Mountains (region A), the glacial area and ice volume were both reduced by 37% between the two periods. The glacial area and ice volume in the Tianshan Mountains (C region) decreased by 19.2% and 16.6%, respectively, while in the Kunlun Mountains (G region), each decreased by 9.9% and 10.2%, respectively, between the two periods. Conversely, the glacier area and ice volume in the Qangtang Plateau (F region) slightly increased by 3.4% and 4%, respectively, between the FGI and SGI periods.

In recent decades, some studies have reported glacier area changes in XJ and its surrounding areas (Sorg et al., 2012; Farinotti et al., 2015; Huai et al., 2015, 2017; Wang et al., 2019; Yao et al., 2019a; Farinotti et al., 2020). Global warming has accelerated glacial shrinkage in XJ, and the glacier retreat rate increased after the 1990s (Li et al., 2011; Sorg et al., 2012; Farinotti et al., 2015). Wang et al. (2019) conducted a comprehensive assessment of changes in the glacier area and mass balance in the third pole region, including XJ. They summarized that most XJ glaciers exhibited significant shrinkage, as evidenced by the decreases in the glacier length and area, as well as mass loss. The rate of glacier retreat was inhomogeneous in XJ owing to climate variability and differences in the local environment and topography. The retreat rate was approximately 0.4%/year in the east Altai, east Kunlun, and Tianshan Mountain and less than 0.2%/year in western Kunlun, Pamir, and Karakoram from the 1970s to the 2010s. Surprisingly, glaciers in central Karakoram were moderately stable, with a shrinkage rate of only 0.04% per year (Wang et al., 2019). The glacier mass balance reflected the coordinated changes; the mass gain or less mass loss occurred in Karakoram, west Kunlun, and Pamir ("Karakoram anomaly"; Hewitt, 2005; Bolch et al., 2012, 2017; Kääb et al., 2012; Zhu et al., 2018; Farinotti et al., 2020), but glaciers in other regions exhibited accelerated mass loss, especially in the 21st century (Wang et al., 2019; Farinotti et al., 2020). Chen et al. (2016) found that approximately 97.52% of the glaciers in Tianshan had retreated from the 1960s to 2010s, and the glaciers in North and East Tianshan experienced accelerated degradation rates since 2000.

There are only a few monitored glaciers in XJ and its surrounding regions. Urumqi Glacier No. 1 (UG1) is a globally referenced glacier in the World Glacier Monitoring Service Network (Li et al., 2011). The equilibrium line altitude, which directly controls the change in the glacier mass balance and area, has risen by approximately 110 m in UG1 since the 1960s (Ye et al., 2016). The annual mass balances of UG1 exhibited an accelerated mass loss at a rate of −345 mm/year from 1960 to 2018 (Fig. 9; China Meteorological Administration (CAM), 2019) and experienced two accelerated melting processes: −81 mm/year during 1960–1984 and −273 mm/year during 1985–1996, which further increased the change rate to −684 mm/year from 1997 to 2018 (China Meteorological Administration (CAM), 2019). The length changes of UG1 retreated during 1959–2018. During 1959–1993, the terminus of UG1 demonstrated a constant decrease at a rate of −4.5 m/year, and the glacier separated into east and west branches in 1993 (Li et al., 2011). The glacial retreat of UG1 has increased since 1993 at rates of −4.7 m/year and −5.7 m/year in the east and west branches during 1993–2018, respectively (Fig. 9; China Meteorological Administration (CAM), 2019).

4.2. Decreases in snow cover and snowfall fraction

Snow cover is a key component of the cryosphere that is critical for hydrological processes, and its change directly influences water resources in arid and water-limited regions (Barnett et al., 2005; You et al., 2020). The most persistent snow cover in XJ is located in the north and northwest, which corresponds well with the high-elevation mountains, including the Altai and Tianshan Mountains (Wang et al., 2020c). Aizen et al. (1997) reported that the maximum snow depth and snow cover duration decreased in the Tianshan Mountains from 1940 to 1991. Based on daily snow depth data, Wang et al. (2020c)also found that snow cover days in XJ exhibited a significant decrease at a rate of 0.19 d/decade during 1961–2017. Spatially, the number of snow cover days in Tianshan decreased significantly, with a rate of 0.78 d/decade. The MODIS data reveal that snow cover decreased in the Tianshan Mountains from

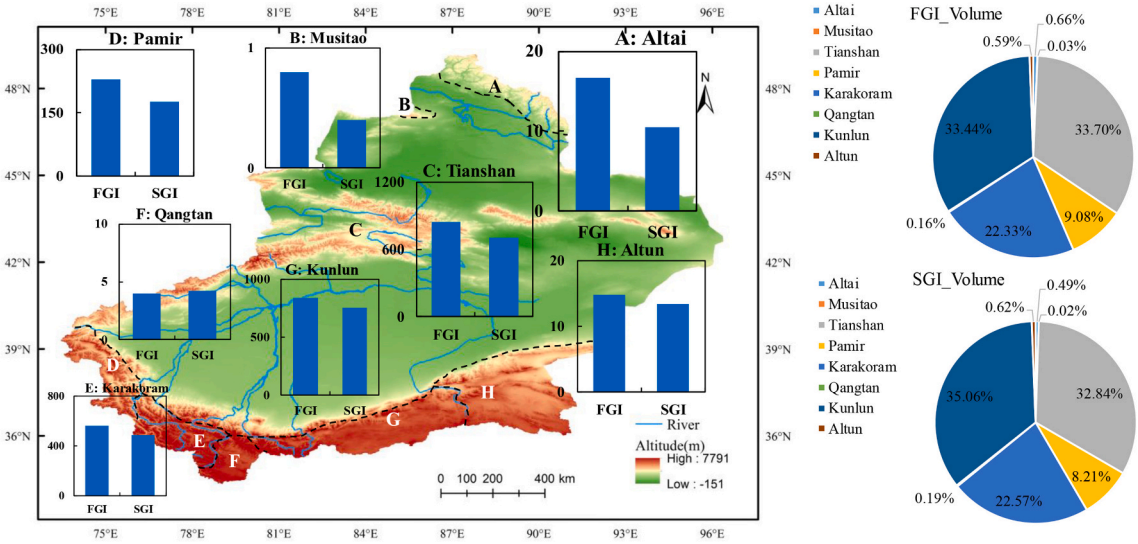

Fig. 8. Same as Fig. 7 but for glacier volume change from FGI to SGI in XJ (x-axis is glacier inventory and y-axis is glacier area, unit: km^3).

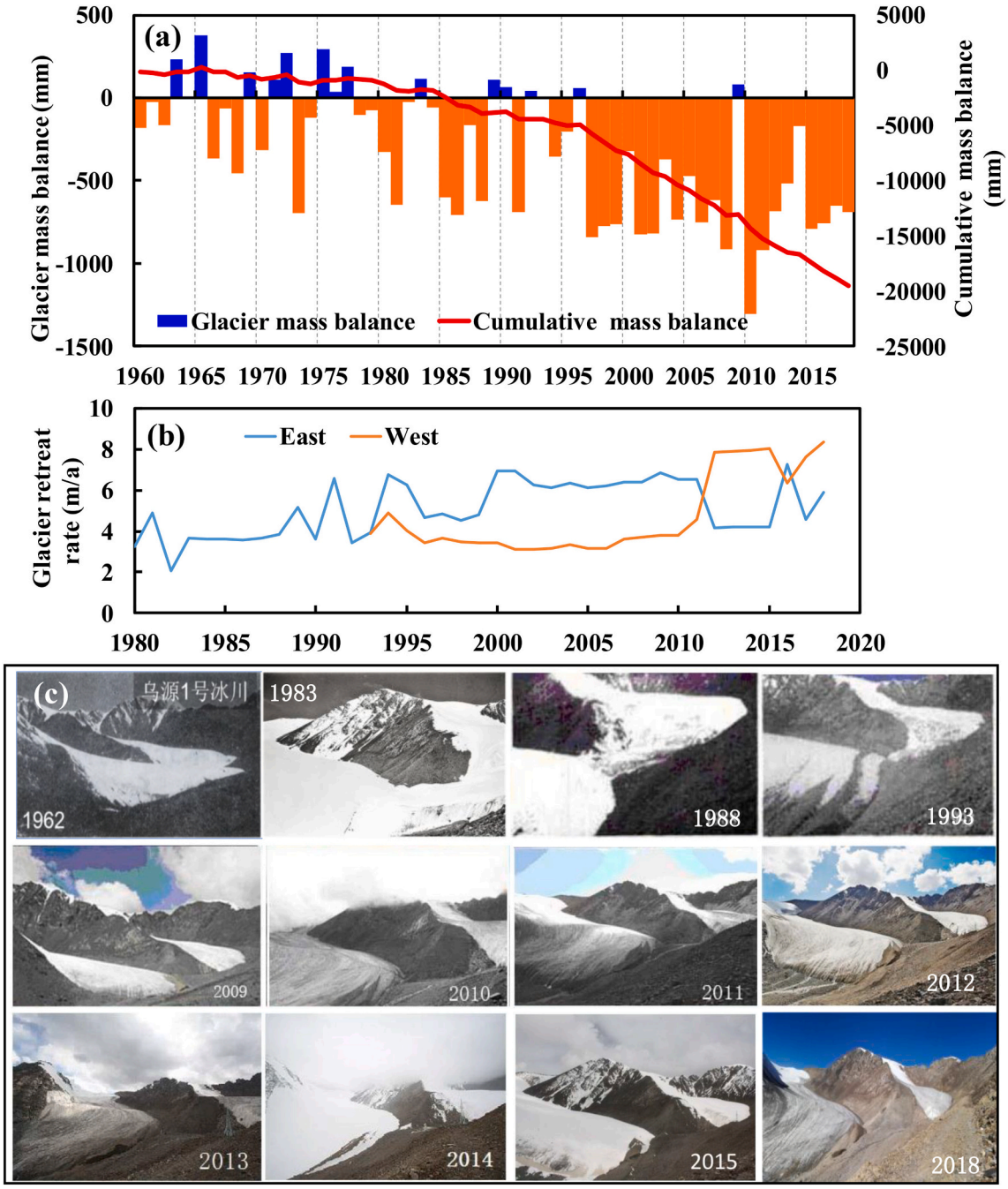

Fig. 9. (a) Glacier mass balance change in the Urumqi Glacier No. 1 (UG1) during 1961–2018. (b) Glacier retreat rate of the east and west branches in the UG1 during 1993-2018 (modified from China Meteorological Administration (CAM), 2019). (c) These photos provided by the Daxigou Mereological Station of Xinjiang Meteorological Bureau and the Tianshan Glaciological Station, Chinese Academy of Sciences.

2002 to 2013 (Chen et al., 2016). Similarly, a decrease in snow cover area was also evident in Altai Mountain from 2001 to 2014 (Chen et al., 2017).

The snowfall fraction, as the ratio of snowfall to precipitation, is a valuable indicator of climate change (Serquet et al., 2011; Li et al., 2020a). Changes in the snowfall fraction directly influence glacial accumulation and ablation, as well as runoff and water resources in mountainous areas (Li et al., 2020a). The multi-source dataset indicated a decrease in the snowfall fraction in the Tianshan Mountains (Guo and Li, 2015; Chen et al., 2016; Li et al., 2020a). The snowfall fraction increased by a rate of 0.6%/decade from 1960 to 1997 but has decreased since 1998 at a rate of 0.7%/decade (Li et al., 2020a), with the primary distribution in the middle elevations (1500–2500 m) (Guo and Li, 2015; Li et al., 2020a). The decreasing snow cover and snowfall fraction confirmed the decrease in snowfall in the mountainous region due to climate warming.

4.3. Runoff increase

River runoff has changed considerably in the arid and cold regions of China during climate warming (Yao et al., 2019b; Li et al., 2019). With increasing temperatures and precipitation, the runoff at most hydrological stations in XJ increased, while others decreased during 1960–2000 (Fig. 10). The observed runoff of seven of eight rivers from the Tianshan Mountains exhibited an increase by 0.27×10^8 m^3/decade (Kashi River) to 1.42×10^8 m^3/decade (Tuoshigan River), while that of

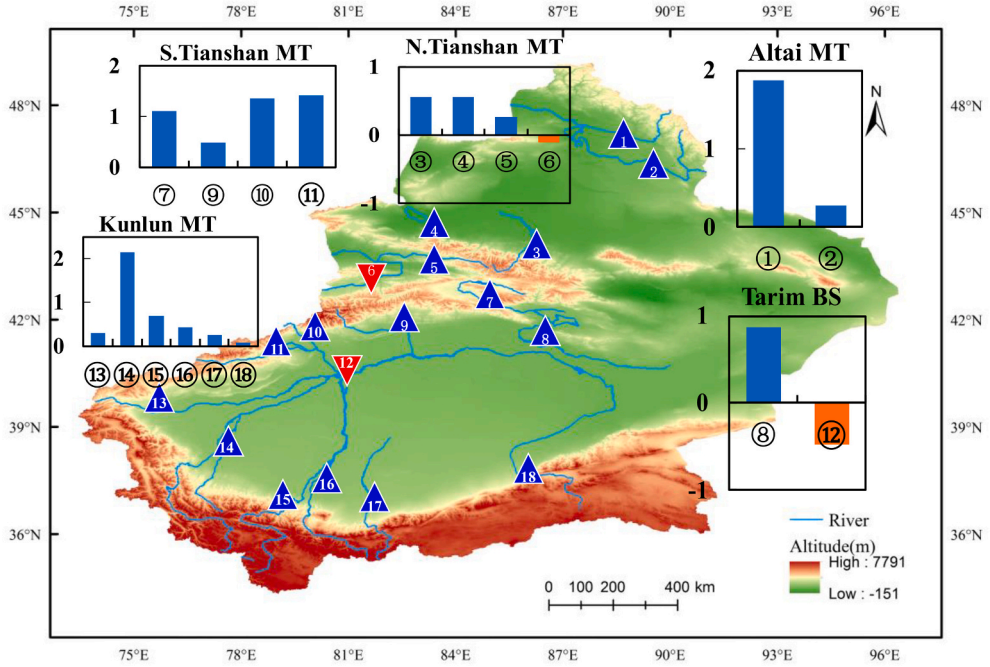

Fig. 10. Spatial distribution of runoff change rate for major rivers in study region (x-axis is the river number, and y-axis is annual change rates of runoff, unit: 10^8 m^3/10a). Rivers are numbered 1–18 based on the following studies: **1.** Burqin River (1957–2008, Qin et al., 2016). **2.** Ulungur River (1960–2010, Qin et al., 2016). **3.** Manasi River (1956–2006, Tang et al., 2011). **4.** Jinghe River (1957–2012, Yao et al., 2015). **5.** Kashi River (1956–2000, Qin et al., 2016). **6.** Tekes River (1956–2000, Qin et al., 2016). **7.** Kaidu River (1958–2017). **8.** Kunque River. **9.** Weigan River (1956–2006, Qin et al., 2016). **10.** Kunmalike River (1957–2017). **11.** Tuoshigan River (1957–2017). **12.** Tarim River (1957–2017). **13.** Kashgar River (1957–2017). **14.** Yarkant River (1957–2017). **15.** Karakash River (1957–2017). **16.** Yulongkash River (1957–2017). **17.** Keriya River (1957–2009, Ling et al., 2012). **18.** Cherchen River (1956–2006, Aynur et al., 2010).

the Tekes River (main headwater sub-catchments of the Ili River) decreased by 0.11 × 10^8 m^3/decade during 1956–2000. As indicated in Fig. 10, all the rivers from the Kunlun Mountains exhibited a significant increasing trend from 0.07 × 10^8 m^3/decade (Cherchen River) to 2.15 × 10^8 m^3/decade (Yarkant River), and a runoff increase was recorded in the Altai Mountains. In rivers on the plain, runoff increased in the Kunquehe River during 1960–2015, while that of the main stream of the Tarim River decreased by 0.48 × 10^8 m^3/decade during 1957–2017. The combined effects of increased precipitation and meltwater have led to increased runoff in XJ since the 1980s (Chen et al., 2015). Increasing regional scale runoff in northern XJ is primarily affected by increasing precipitation, while it is dominated by increasing meltwater from

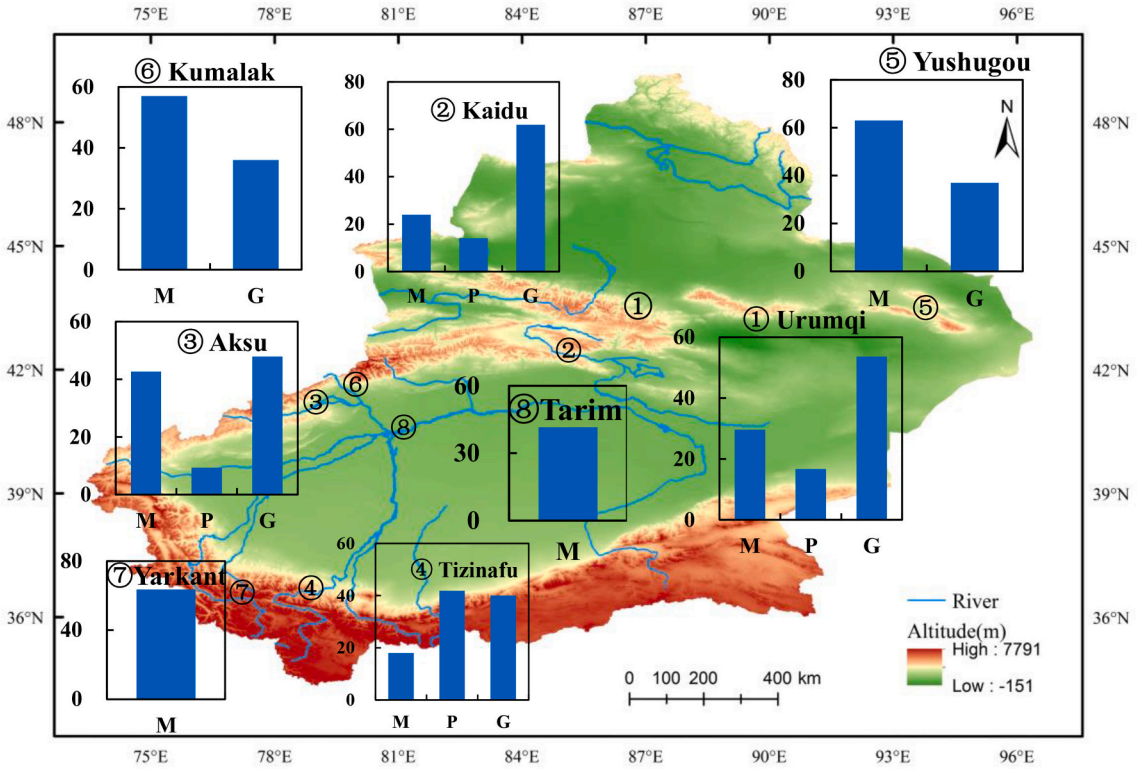

Fig. 11. Proportions of changed runoff in the study region (x-axis is the runoff component, and y-axis is the proportion of various water sources for runoff, unit: %; **M** is glacier snow meltwater, **P** is precipitation, and **G** is groundwater). Rivers are numbered 1–8 based on the following studies: **1.** Urumqi River (Sun et al., 2016a). **2.** Kaidu River (Sun et al., 2016b). **3.** Aksu River (Sun et al., 2016b). **4.** Tizinafu River (Fan et al., 2015). **5.** Yushugou River (Wang et al., 2015). **6.** Kumalak River (Kong and Pang, 2012). **7.** Yarkant River (Gao et al., 2010). **8.** Tarim River (Gao et al., 2010).

temperature changes in southern XJ (Wang et al., 2013a; Chen et al., 2015, 2019a).

The runoff component in arid regions includes glacier snow meltwater, precipitation, and groundwater (Chen et al., 2015, 2019a). Fig. 11 shows the proportions of the changed runoff components in the eight typical river basins of XJ. In central Tianshan, meltwater accounted for 29.6% and 24% of the runoff in the Urumqi River and Kaidu River (Sun et al., 2016a, 2016b). In the western Tianshan and Kunlun Mountains, 42%–64% of the runoff was derived from meltwater. In addition, the contribution of meltwater to runoff increased in most rivers in XJ under climate warming. For example, the meltwater proportion in the Tarim River during 1961–2006 increased from 41.5% to 46.5% after 1990 (Gao et al., 2010).

The river runoff changes are not only linked to temperature, precipitation, and evapotranspiration, but also to modifications in underlying land surface conditions caused by human-induced effects (Hu et al., 2021). In general, the long-term runoff of high mountains rivers is mainly controlled by climate change, while the human activities dramatically affected the runoff changes in rivers sources in medium-to-low mountains (Chen et al., 2019b). Previous studies have reported the runoff change attributions in different rivers across the XJ. For instance, the relative contribution of climate change to runoff increase was 90.5% of the Kaidu River (Chen et al., 2013b), and the contribution rate of 94% in the Aksu River (Li et al., 2016a). Additionally, the relative contribution of human activities to runoff reduction surpassed 60% in the Tarim River mainstream, with water consumption impacted runoff changes the most ((Chen et al., 2019b)). For the Jinghe River, the contribution of human activities to runoff change was 85.7% during 1980-2011 (Dong et al., 2015). These study findings provide essential information for water resource management in XJ region.

4.4. Lake expansion

Inland lakes are key indicators of climate change and serve as a link between the land and the atmosphere by means of water and energy exchange (Mason et al., 1994; Ma et al., 2007; Li and Morrill, 2013; Li et al., 2019). They can also provide crucial water resources for agriculture, ecosystems, and human welfare in water-limited regions (Yao et al., 2018d; Zhang et al., 2020). XJ lakes comprise approximately 13.2% of China's lake area, with a total lake area of 1.24 × 10^4 km^2 (as of 2010; lakes with areas > 1 km^2). Some studies have confirmed that most lakes on the TP have undergone rapid expansion during recent decades, especially in the TP interior (Yao et al., 2019a; Wang et al., 2020a; Zhang et al., 2020). Based on Landsat satellite data (TM/ETM+/OL), Li et al. (2018) studied the lake area changes of 33 large lakes (with areas > 10 km^2) in XJ from 2000 to 2014. During the past 15 years (2000-2014), the total lake area in XJ increased from 5,260.9 km^2 to 5,561.1 km^2 at a rate of 11.09 km^2/year (Fig. 12b;Zhang et al., 2018b). Fig. 12a provides the regional differences of lake changes in the XJ during 2000-2014. Most lake areas in northern XJ (A region) exhibited stable changes, and they have expanded significantly in southern XJ (C region, including Tarim Basin, Kunlun Mountain, and Altun Mountain), whereas lakes in central Tianshan (B region) and the Qangtang Plateau (D region) have shrunk (Fig. 12a; Li et al., 2018;Zhang et al., 2018b). Generally, the spatial patterns of alpine lakes have exhibited a significant expansion or stabilization, but have shrunk in the plains and rump lakes, which are influenced by changes in precipitation, meltwater, and human activities. Increased precipitation and enhanced meltwater from the cryosphere are primary contributors to lake expansion in the Tarim Basin and the Kunlun Mountains (Zhang et al., 2017c; Yao et al., 2019a; Wang et al., 2020a; Zhang et al., 2020). Typical lakes include the Ayak Kumu Lake, which exhibited an expansion of 335 km^2 from 2000 to 2014 (51.9% increase) and became the largest lake in XJ (Li et al., 2018). The geological structure of the lake is the main contributor to the stabilized lake changes in northern XJ, followed by meltwater, such as Sayram Lake (Liu et al., 2019; Li et al., 2018) and Kanas Lake (Li et al., 2018). Human activity has caused lake shrinkage in rump lakes via agricultural irrigation, such as Ebinur Lake (Ma and Wang, 2007; Li et al., 2019) and Bosten Lake (Yao et al., 2018d; Li et al., 2018). In addition, reduced precipitation may be responsible for lake shrinkage in the Qangtang Plateau, along with a contribution from reduced meltwater from a slight mass gain (Liu et al., 2015; Li et al., 2018; Farinotti et al., 2020).

Bosten Lake, the largest inland freshwater lake in China, exhibited dramatic changes from 1961 to 2019, with a lake level decrease of 2.7 m during 1961–1987, a rapid increase of 4.4 m during 1988–2002, a

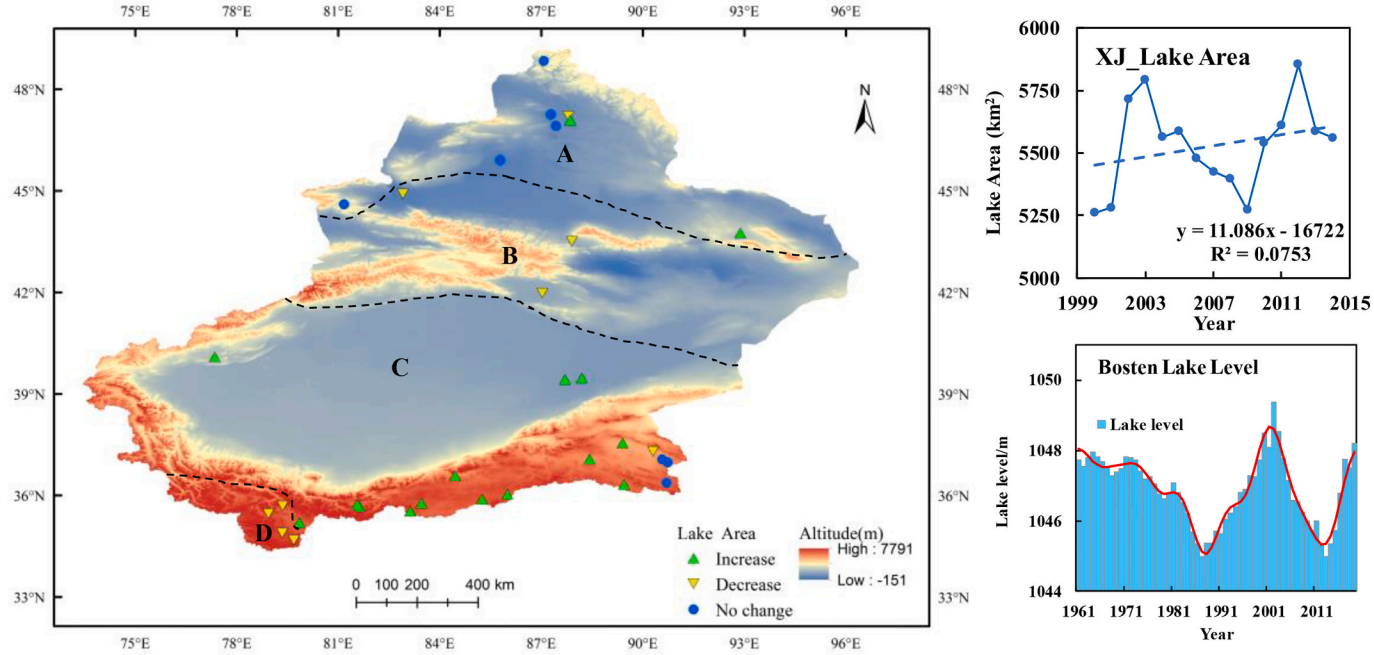

Fig. 12. **(a)** Spatial distribution of lake area changes in study region from 2000 to 2014 (modified from Li et al., 2018). **(b)** Lake area change in XJ from 2000 to 2014 (modified from Zhang et al., 2018b). **(c)** Bosten Lake level change from 1961 to 2019 (modified from Yao et al., 2018d).

drastic 4.4 m decrease during 2003–2013, and a recent increase of 3.2 m since 2013 (Fig. 12c; Yao et al., 2018d). Climate regime shifts and anthropogenic impacts are likely the dominant drivers of the lake area changes. From 1988 to 2002, climate wetting has played a critical role in lake expansion; however, increased irrigation and water conveyance and decreased precipitation were the main drivers of lake retreat during 2003–2013 (Guo et al., 2015; Yao et al., 2018d). In addition, increased precipitation and accelerated glacier meltwater resulted in lake expansion in this region in recent years (2013–2019).

5. Implications of climatic and hydrological changes

5.1. Moisture budget, sources, and contributions to precipitation

Located in the hinterland of the Eurasian continent and north of the TP, moisture in XJ is predominantly transported by the mid-latitude westerlies that flow from the western continent and oceans (Dai et al., 2007; Wang et al., 2007a; Ao and Sun, 2014; Huang et al., 2015). The moisture input mostly occurs across the western boundary, accounting for 69.4% of the total input, and approximately 72% of the moisture output occurs at the eastern boundary (Guan et al., 2019). During 1979–2012, the net moisture budget exhibited an increasing trend in XJ, which was primarily attributed to the increased moisture input across the western boundary transport. Although the southern boundary moisture exhibited a stronger increasing trend (Fig. 13), the total attribution rate was limited to only 3%–7% of the total input (Guan et al., 2019; Yao et al., 2020b). Since approximately 2000, moisture transport has displayed a decreasing trend at the western and eastern boundaries due to weakened westerlies. However, the decrease in moisture transport across the eastern boundary is much greater than that across the western boundary; thus, the net moisture budget still exhibits an increasing tendency (Fig. 13). An anticyclone near Lake Baikal induced an anomalous easterly inflow in XJ and caused a significant decrease in moisture transport across the eastern boundary of XJ, resulting in an increased net moisture budget (Fig. 13; Yue et al., 2020). Yue et al. (2020) found that the anomalous anticyclone near Lake Baikal was regulated by sea surface temperatures (SST) anomalies between the high-latitude Northwest Atlantic Ocean and the Mediterranean Sea. Corresponding to the abnormal warming in the Indian Ocean, another anomalous cyclone appeared in Central Asia, and further triggered moisture from the Indian Ocean across the Iranian Plateau and Central Asia into XJ (Fig. 13; Huang et al., 2015; Zhao et al., 2014, 2019; Chen et al., 2019a; Lu et al., 2019).

Identifying the moisture sources and their contributions is key to understanding the hydrological cycle process at different time scales (Hua et al., 2017; Gimeno et al., 2019). The moisture source–sink relationship is often used to investigate the causes of precipitation and extreme variability at spatiotemporal scales (Gimeno, 2013; Gimeno et al., 2019). Over the past decades, many approaches have been employed to quantitatively implement the moisture source–sink relationship, such as the classical Eulerian (Van der Ent and Savenije, 2011), the Lagrangian model (Draxler and Hess, 1998; Stohl et al., 2008; Stohl and James, 2005; Jiang et al., 2017), moisture recycling model (Brubaker et al., 1993; Schär et al., 1999; Dominguez et al., 2008; Gimeno, 2013), and stable isotope approaches (Dansgaard, 1964).

Table 1 summarizes the key results of the link between precipitation (extremes) and the related moisture source–sink relationship in XJ. In the mid-latitudes of the Northern Hemisphere, westerly winds are the main atmospheric system. The prevailing westerly transport resulting in XJ precipitation originates from the Atlantic Ocean, Arctic Ocean, Black Sea, and Caspian Sea (Yatagai, 2003; Dai et al., 2006; Guan et al., 2019). Zhou et al. (2019) also found that the moisture associated with extreme precipitation was strongly influenced by the westerly winds. Some studies have identified that the moisture sources of XJ precipitation are primarily from the western ocean and the European continents. Other studies have suggested the influence of southern oceanic regions, especially over the southern XJ and Tarim Basin regions (Zhao et al., 2014; Huang et al., 2015). Traditionally, the moisture transported from the Indian Ocean has difficulty reaching the inland XJ region due to the blocking effect of the TP (Ao and Sun, 2014; Zhou et al., 2019). Previous studies have determined that extreme precipitation in the Tarim Basin is closely related to accelerated water vapor transport from the Indian

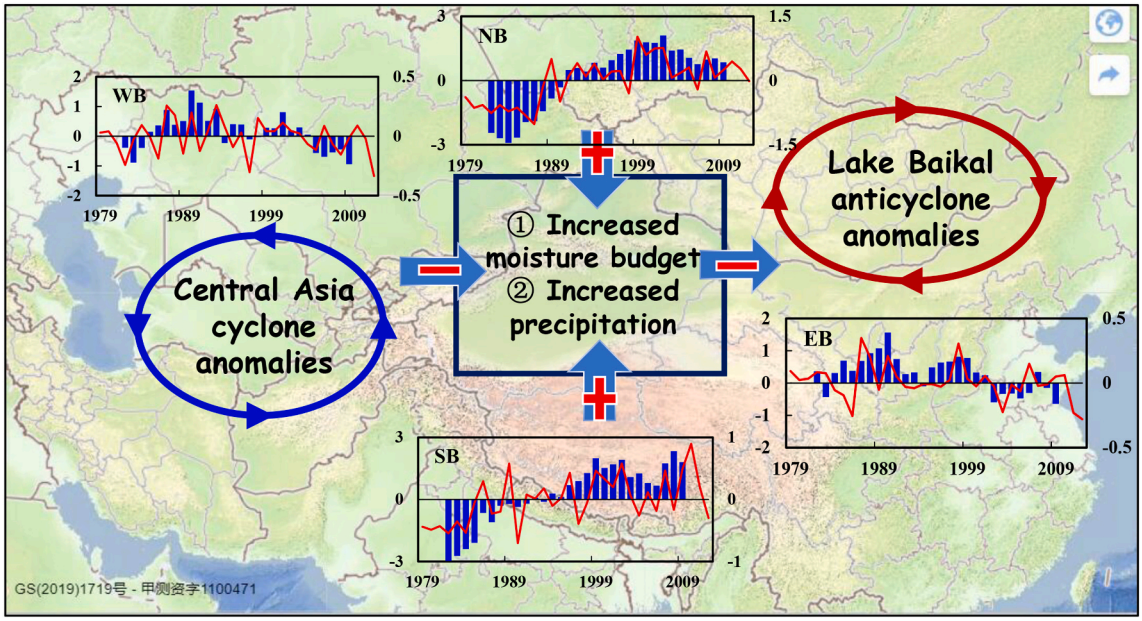

Fig. 13. Schematic diagram illustrating the changes and physical mechanisms of the moisture budget in XJ. The blue box denotes XJ. The arrows indicate the moisture transport paths, and circles denote the upper level geopotential height anomalies. The + and - denotes the increasing and decreasing trends of the moisture flux budget on each boundary. WB, EB, NB, and SB denote the western, eastern, northern, and southern boundary moisture flux budgets, respectively. The red line represents the annual moisture flux budget on each boundary (left ordinate) during 1979–2012, and the blue histogram represents their interdecadal variations from the 7-year running average (right ordinate). The moisture budget for XJ was calculated through vertical integration from 1,000 to 300 hPa using ERA-Interim reanalysis data.

Table 1
Summary of precipitation and extremes associated with atmospheric moisture.

Affected Region	Event/Date	Moisture sources related to	Technique applied	Reference
XJ		Moisture mostly comes from the prevailing westerlies, especially in winter.	Eulerian	Yatagai, 2003
XJ	Precipitation, 1980–2000	Moisture comes from the Atlantic Ocean, Arctic Ocean, Black Sea, and Caspian Sea; moisture sources vary seasonally.	Eulerian	Dai et al., 2006
Tarim Basin, southern XJ	Summer precipitation, 1961–2010	Moisture originates from the Indian Ocean.	Eulerian	Zhao et al., 2014
Tarim Basin, southern XJ	Summer precipitation, 1961–2009	Moisture comes from the Arabian Sea transported through the eastern periphery of the Tibetan Plateau.	Eulerian	Huang et al., 2015
Northern XJ	Precipitation events during 2012–2013	Contribution rates of recycled moisture vary from 3.4% to 16.2% in different oases, for example, approximately 16.2% for Urumqi.	Stable isotope approach	Wang et al., 2016
Tianshan Mountain	Precipitation, 2000–2010	Local evaporation contributed to 8–9.32% of the total amount.	Precipitation recycling model and stable isotope approach	Yao et al., 2016b
Northern XJ	Summer extreme precipitation, 1951–2014	North Atlantic Ocean, Arctic Ocean, Indian Ocean, and Eurasia are the predominant moisture sources.	Lagrangian	Huang et al., 2017b
Northern XJ	Summer precipitation, 1982–2010	96% of moisture originates from land evaporation in Central Asia, western Siberia, and eastern and northeastern Europe.	Lagrangian and dynamic recycling model (DRM)	Hua et al., 2017
Eastern XJ	Extreme precipitation event, 15–18 July 2007	The moisture sources in the Atlantic Oceans and Central Asia contributed 37% and 44%, respectively.	Lagrangian (HYSPLIT)	Yao et al., 2018c
XJ	Summer precipitation, 1979–2012	Moisture comes from high latitudes of the European continent.	Eulerian	Guan et al., 2019
XJ	Monthly precipitation, 1961–2015	The annual precipitation recycling ratio fluctuates between 4% and 10% and exhibits an increasing trend.	Eulerian and precipitation recycling model	Wu et al., 2019
XJ	Extreme precipitation, during April–September of 2008–2015	Moisture is mostly transported by westerly winds. XJ and Central Asia are key moisture sources for the development of extreme precipitation, and local contributions account for 40% and 70% in Ili Valley and Hami area, respectively.	Lagrangian (FLEXPART)	Zhou et al., 2019
XJ	Precipitation, 1961–2010	The annual precipitation recycling ratios were 6.48% and 7.79% for the two models.	Eulerian and precipitation recycling model	Yao et al., 2020b
XJ	Monthly precipitation, 1979–2018	(a) Three similar moisture transport paths in winter and summer months, and one more path in summer. (b) Contribution rate of XJ itself and Central Asia accounts for more than 80%, among which the local contributions account for 52%.	Lagrangian (FLEXPART)	Yao et al., 2020d
Hami, Eastern XJ	Extreme precipitation event, 31 July 2017	Moisture from the South China Sea was transported by an easterly moisture relay transmission.	Eulerian and Lagrangian	Liu et al., 2020

Ocean and the Arabian Sea (Yang and Zhang, 2007; Yang et al., 2012; Zhao et al., 2014; Huang et al., 2015; Zhang et al., 2018a). For example, Zhao et al. (2014) found that water vapor originating from the Indian Ocean could be transported to XJ through the valley between the TP and the Iranian Plateau for summer precipitation. Huang et al. (2017b) proposed that moist air from the Arabian Sea is transported through the astern periphery of the TP into XJ causing extreme summer precipitation. However, external continental evaporation and local moisture recycling also have a strong impact on precipitation in inland regions (Drumond et al., 2011; Hua et al., 2017; Zhou et al., 2019). Hua et al. (2017) found that 96% of the moisture related to summer precipitation in XJ originates from external continental evaporation in Central Asia, western Siberia, and Europe. Zhou et al. (2019) indicated that XJ and Central Asia are the primary sources of moisture for the development of extreme precipitation, and local recycling contributions account for 40% and 70% in the Ili Valley and Hami area, respectively. Yao et al. (2020d) also determined that more than 80% of the moisture that was correlated with the summer precipitation in XJ had originated from land evaporation in XJ and Central Asia, and local moisture recycling accounted for 52%.

5.2. Acceleration of local precipitation recycling in mountain–basin system

Local precipitation recycling plays a key role in balancing the hydrological and energy cycles and contributes to local and remote precipitation due to evaporation from land and water surfaces and plant transpiration (Dominguez et al., 2008; Gimeno, 2013; Gimeno et al., 2019; Zhao et al., 2014; Van der Ent and Savenije, 2011). Some studies have indicated that precipitation recycling is accelerating due to enhanced evaporation associated with a warmer climate, which has strongly affected hydrological cycles (Li et al., 2019; Yao et al., 2020b). Van der Ent and Savenije (2011) found that approximately 40% of land precipitation originates from terrestrial evaporation. In XJ, local precipitation recycling significantly contributes to extreme precipitation events (Zhou et al., 2019; Yao et al., 2020d); however, precipitation recycling accounts for less than 10% of the total annual precipitation and varies regionally (Yao et al., 2020b). Yao et al. (2016b) demonstrated that precipitation recycling in the Tianshan Mountains accounted for 9.32% of the annual precipitation. Wang et al. (2016) proposed that the precipitation recycling rate was 16.2% in Urumqi and less than 5% in the Shihezi and Caijiahu Oases. Despite the relatively low contribution rates of precipitation recycling, it is essential for precipitation in arid regions (Li et al., 2018).

Climate warming and wetting in XJ can enhance local precipitation recycling. The contribution rate of precipitation recycling in XJ increased remarkably at a rate of 0.44–0.53%/decade during 1961–2010 (Yao et al., 2020b). Wu et al. (2019) also found that the contribution increased during 1961–2015 at a rate of 0.3%/decade. Precipitation recycling may increase precipitation in a warming climate. In addition to climate warming, human water use (e.g., irrigation and reservoirs) has altered the spatiotemporal distribution of surface water and induced land water–to–atmosphere interactions, which may affect the local and remote precipitation. Some studies have confirmed that irrigation can increase both local and remote precipitation (Stidd, 1975; DeAngelis et al., 2010; Lo and Famiglietti, 2013; Alter et al., 2015).

Fig. 14a summarizes the mechanistic framework of the influence of irrigation on the increase in precipitation. We also propose a schematic diagram of the mountain–valley breeze circulation effect on the precipitation increase in the mountain–basin system of XJ. Oasis irrigation has been increasingly practiced and rapidly developed in XJ recently (Yao et al., 2020b). Irrigation can increase soil moisture and enhance the

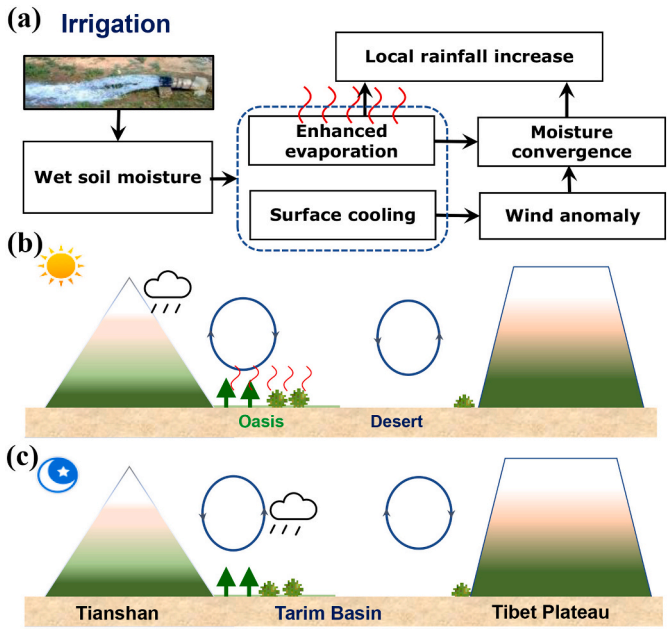

Fig. 14. Framework for increasing rainfall due to irrigation in the mountain–basin system. A mechanistic pathway from irrigation to rainfall increase (a). A schematic diagram of the valley breeze circulation (b) and mountain breeze circulation (c) for the mountain–basin system (modified from Yao et al., 2020b).

atmospheric moisture. During the daytime, the valley breeze can transport moisture from the oasis to the mountain region, increasing mountainous moisture by enhancing the upward vertical motion and precipitation in the mountain regions (Fig. 14b). At night, the mountain breeze blows from the mountains to the oasis and can cause increased precipitation in the oasis region (Fig. 14c).

5.3. Aggravation of meteorological drought and adverse ecological effects

Global warming and hydrological changes can influence regional drought and vegetation dynamics, especially in XJ regions (Chen et al., 2015). The observed temperatures and precipitation have changed dramatically in XJ during the past few decades. Based on the SPI and Standardized Precipitation Evapotranspiration Index (SPEI)), Yao et al. (2018a) comprehensively assessed the multi-scale variations in drought in XJ and found that the climate has demonstrated a significant warming–wetting trend during 1986–1997, after which the climate has shifted from wet to dry, implying the aggravated meteorological drought in XJ. Aggravated drought is mostly controlled by changes in evaporative demand, and it has risen due to global warming (Vicente-Serrano et al., 2010), which may have adverse ecological effects. Recent studies have reported that soil moisture in XJ has exhibited a sharply decreasing trend since the mid-1990s, with an average moisture reduction of 42.2% (Zhang et al., 2016; Yao et al., 2018a). Changes in soil moisture are correlated with climate change (Yang et al., 2010). Vegetation coverage and the normalized difference vegetation index (NDVI) increased during 1982–1997 and has decreased since 1997 (Wang et al., 2013b; Yao et al., 2018a, 2018b). The total net primary production (NPP) has also exhibited a decrease in XJ since 2000 (Fang et al., 2013). Vegetation dynamics have been closely related to climate change in recent decades. The increased temperatures and precipitation may have conjointly

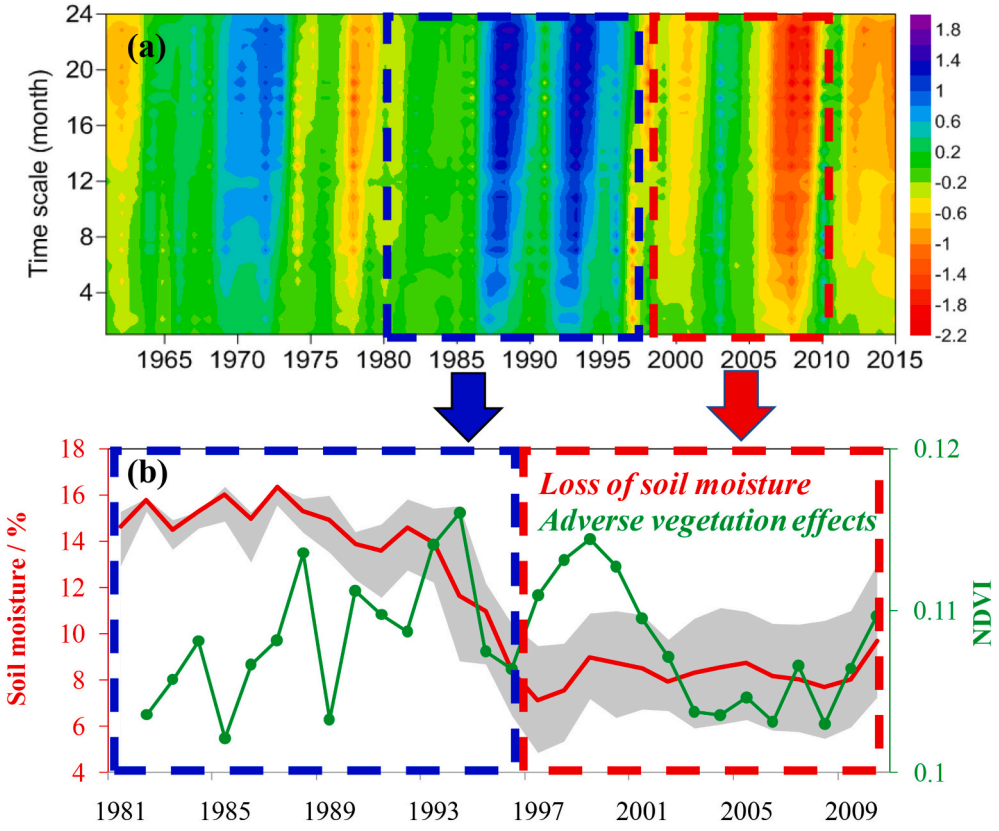

Fig. 15. **(a)** Change in SPEI at different timescales (1 to 24 months) in XJ during 1961–2015. **(b)** Evolution of soil moisture (red solid line) and vegetation NDVI (green solid line) in XJ during 1982–2010. Red dotted line represents the warm–humid climate during 1985–1997; blue dotted line represents the climatic wet–to–dry shift since 1997. Gray shadow represents soil moisture at each depth (0–50 cm) in XJ.

caused a warming–wetting climate, leading to increased soil moisture and vegetation greening during 1985–1996. However, intensified warming, higher PET, and diminished precipitation may have caused increased soil moisture loss, thereby reducing vegetation cover since 1997, intensifying the unreliability and vulnerability of the ecosystem (Fig. 15). In addition, Yao et al. (2018b) suggested that the decrease in the vegetation NDVI may have been triggered by climate extremes increases in XJ since 1997.

5.4. Shrinkage of the desert-oasis ecotone

The desert-oasis ecotone (DOE), a boundary and corridor between the oases and deserts, plays a prominent role in controlling the material and energy exchange between the oases and deserts, as well as maintaining the security and stability of the oases and desert ecosystems (Wang et al., 2007b; Pi et al., 2017; Zhang et al., 2017b; Wang et al., 2020b). DOEs are also highly sensitive to climate change and human activity (Neilson, 1993; Chen et al., 2020). The XJ has been severely affected by desertification and has been exhibiting severe sandy desertification with increasing improper human intervention over the last decades (Dittrich et al., 2010). For several decades, a large area of the DOE zone in XJ has been reclaimed for cropland and continuous cotton production (Li et al., 2020b). The land cover change demonstrated that the area of the DOE zone in XJ experienced a significant decrease (−43%), while the oasis increased continuously (+35%) during 1990–2008 (Amuti and Luo, 2014). In the Tarim River basin, the DOE area was continuously reduced at a rate of 12.4% per decade, and the NDVI value in the DOE area also decreased by 0.015 from 1990 to 2015 (Chen et al., 2020). The DOE area exhibited continuous shrinkage, whereas the oasis in the XJ exhibited notable growth. These changes have been induced primarily by land and water exploitation. The accelerated oasification process can extract more groundwater, resulting in a sharp decline in the groundwater levels and dehydration of the shallow roots of the desert plants (Chen et al., 2020). These changes have reduced biodiversity and vegetation coverage, affecting the ecological barrier function in the DOE zone. Thus, the DOE changes have been affected by both oasification and desertification processes, and mutual feedback between both processes has been determined by the spatiotemporal pattern of the desert oasis environment (Fig. 16). In addition, water directly controls the dynamic balance between both processes and vegetation dynamics in the transitional zone and is critical for the sustainable development of desert–oasis environments (Xue et al., 2019).

6. Conclusions and perspectives

Climate change has caused rapid changes in recent decades in XJ, China. In this paper, we provide a systematic review of recent climate changes in this region and its effects on the hydrological system changes (see Fig. 17). We also proposed a theoretical framework of the climate and human activity influence on hydrological changes in mountain–basin system (Fig. 18), and enhances our scientific understanding of arid region hydrology in the future. The key findings are summarized as follows:

(1) XJ rapidly warmed by 0.30 °C/decade ($p < 0.01$) during 1961–2018, and the strongest warming was observed in winter (0.42 °C/decade, $p < 0.01$). Climatic warming has resulted in increased warm extremes and decreased cold extremes. The annual total precipitation and related extremes have significantly increased but have exhibited strong interannual variations since the 21st century. Moreover, the enhanced evaporation implies an accelerated water transformation from liquid to gas in arid XJ.

(2) Climate warming has directly affected the hydrological system in XJ, leading to glacier retreat, decreases in snow cover and the snowfall fraction, as well as increased recycling precipitation, increased river runoff, and lake expansion. The retreat rate increased for almost all the glaciers after the 1990s, while the glaciers in central Karakoram were moderately stable. The combined effects of increased precipitation and meltwater have led to increased runoff in XJ since the 1980s. The decrease in both the snow cover and snowfall fraction caused a decrease in snowfall in the mountainous region of XJ. Regarding the lake area changes, the alpine lake areas significantly increased or were maintained compared with plains and rump lake areas, which significantly decreased.

(3) Warmer climate and related changes in hydrological regimes may threaten water availability in arid XJ, which has direct implications for water resources and ecological security. The SPEI indices revealed that the climate experienced a wet-to-dry shift since 1997, resulting in an aggravated meteorological drought in XJ, which may cause adverse ecological effects, such as increased soil moisture loss, reduced vegetation cover, and DOE shrinkage. These factors can intensify the unreliability and vulnerability of water resources and ecosystems in XJ.

As achievements in the study of climate and hydrological changes have become increasingly detailed, some new perspectives and unresolved questions regarding changes in XJ were identified as follows:

(1) Do reanalyses, remote sensing, and climate models accurately reproduce climate variability in mountain basin systems? The sparse and incomplete surface observations in XJ, coupled with a unique mountain–basin structure and mountain–desert environment, limit the

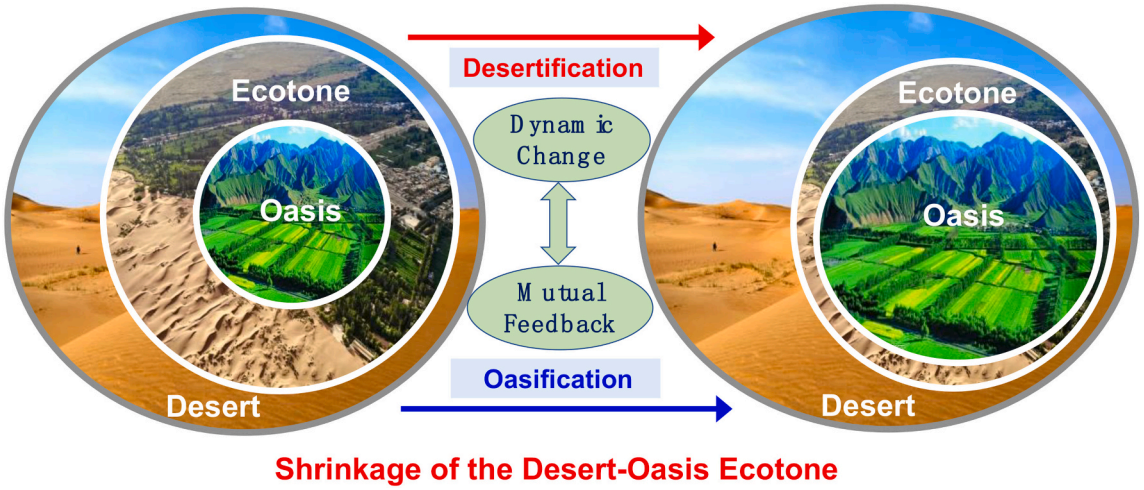

Fig. 16. Schematic diagram of DOE shrinkage

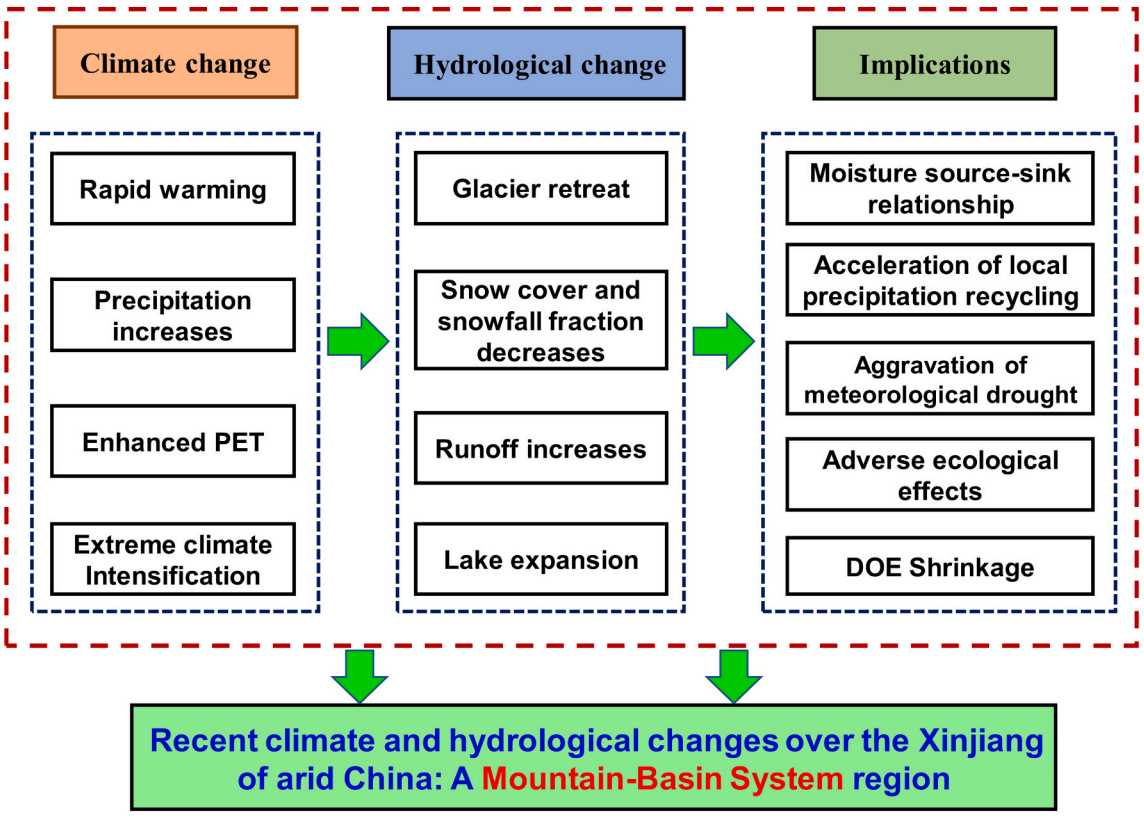

Fig. 17. Conceptual model of climate and hydrological changes in XJ, China

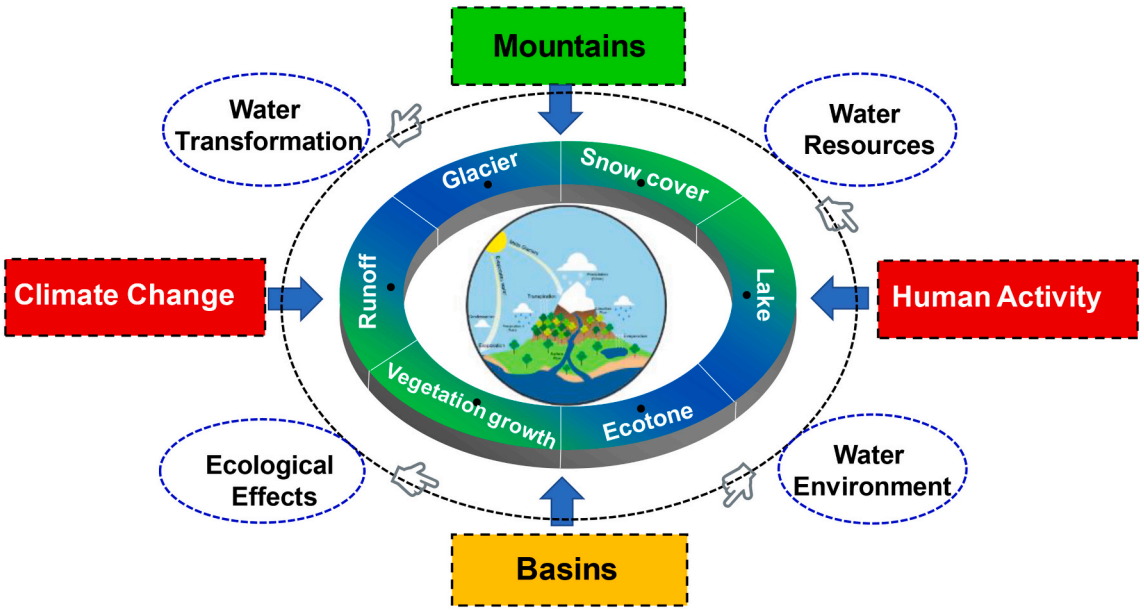

Fig. 18. Theoretical framework of the climate and human activity influence on hydrological changes in mountain–basin system

reproduction of climate change findings, particularly regarding precipitation. Less than 10% of the territory has observation stations. Thus, the use of multiple datasets to investigate climate variability is critical in XJ. Although multiple datasets have been employed to reveal climate variability in XJ and its surroundings (Yao et al., 2020c), the discrepancies among different products are not well known. Thus, it is necessary to systematically evaluate multiple products and explore climate variability in XJ.

(2) Where does the moisture in arid XJ originate, especially the moisture that influences extreme precipitation? Generally, the mean annual precipitation and moisture conditions are exceptionally low in XJ because they are far from oceanic moisture sources (Yao et al., 2020b). However, extreme rainstorm events have occurred frequently in the driest regions in recent years (Zhao et al., 2014; Liu et al., 2020). For instance, a sudden extreme rainstorm event occurred in Hami (located in eastern XJ) on July 31, 2018, in which the 12-h accumulated

precipitation reached 110 mm (annual precipitation of 50 mm) (Liu et al., 2020). It is critical to quantify the moisture sources, transport processes, and paths associated with extreme precipitation.

(3) What determines the decadal climatic transition in XJ, and what are the physical mechanisms of the action? Since the mid-1980s, air temperatures and precipitation have increased rapidly in XJ, reflecting the warming–wetting trend (Shi et al., 2003, 2007; Li et al., 2012; Wu et al., 2019; Wang et al., 2020). However, a drying trend has been found in northern China (including XJ) since the 2000s (Ma et al., 2018; Yao et al., 2018a). Although many physical mechanisms have been proposed to explain these transitions, including the El Niño–Southern Oscillation (ENSO), Atlantic Multidecadal Oscillation (AMO), East Asia-Pacific teleconnection pattern (EAP), and the Indian Ocean (Zhao et al., 2006; Yang et al., 2018; Yang and Zhang, 2007; Zhao and Zhang, 2016; Huang et al., 2015), these interaction processes remain unclear.

(4) How will climatic and hydrological changes respond to 1.5 °C and 2 °C mean global warming? Recent studies have focused predominantly on changes in future climate and extreme climate scenarios (Shi et al., 2007; Wang and Chen, 2014; Doris et al., 2016; Guo and Shen, 2016). Based on CMIP5 projections, the temperature increase in northern XJ could exceed 3 °C during 2046–2075 (relative to 1971–2100) (Guo and Shen, 2016), and precipitation has been projected to increase by up to 5%–10% in northwestern China (Wang and Chen, 2014). However, studies have rarely examined future climatic conditions that are correlated with hydrological changes in XJ and the discrepancies between 1.5 °C and 2 °C global warming.

(5) How can we assess the increased hydrometeorological disaster risks under warming climate conditions? The XJ is highly vulnerable to hydro-meteorological disasters such as storm floods, droughts, snow avalanches, glacial lake outbursts, debris flows, and snow disasters. Infrastructure in arid regions is less well-adapted to extreme events (Donat et al., 2016). To protect human lives and major infrastructure, it is necessary to quantitatively assess the relationship between hydrometeorological changes and hazard triggers and develop an approach for hazard assessments.

Declaration of Competing Interest

The authors declare that they have no known competing financial interests or personal relationships that could have appeared to influence the work reported in this paper.

Acknowledgments

This work was funded by the National Key Research and Development Program of China (2018YFA0606403), National Natural Science Foundation of China (U1903113) and National Key Research and Development Program of China (2019YFC1510501).

References

Aizen, V.B., Aizen, E.M., Melack, J.M., Dozier, J., 1997. Climatic and hydrologic changes in the Tien Shan, Central Asia. J. Clim. 10 (6), 1393–1404. https://doi.org/10.1175/1520-0442(1997)010<1393:CAHCIT>2.0.CO;2.

Aizen, E.M., Aizen, V.B., Melack, J.M., Nakamura, T., Ohta, T., 2001. Precipitation and atmospheric circulation patterns at midlatitudes of Asia. Int. J. Climatol. 21, 535–556.

Alter, R.E., Im, E.S., Eltahir, E.A., 2015. Rainfall consistently enhanced around the Gezira Scheme in East Africa due to irrigation. Nat. Geosci. 8 (10), 763.

Amuti, T., Luo, G., 2014. Analysis of land cover change and its driving forces in a desert oasis landscape of Xinjiang, northwest china. Solid Earth 5 (2), 1071–1085.

Ao, J., Sun, J.Q., 2014. Difference of water vapour transportation in the interannual and decadal variations of winter precipitation over western China (in Chinese). Climatic Environ. Res. 19, 497–506.

Aynur, M., Wahap, H., Yang, X.D., 2010. The climatic changes of Qarqan river basin and its impact on the runoff. Xinjiang Agric Sci 47, 996–1001.

Barnett, T.P., Adam, J.C., Lettenmaier, D.P., 2005. Potential impacts of a warming climate on water availability in snow-dominated regions. Nature 438, 303–309.

Bolch, T., et al., 2012. The state and fate of Himalayan glaciers. Science 336, 310–314.

Bolch, T., Pieczonka, T., Mukherjee, K., Shea, J., 2017. Brief communication: Glaciers in the Hunza catchment (Karakoram) have been nearly in balance since the 1970s. Cryosphere 11, 531–539.

Brubaker, K.L., Entehabi, D., Eagleson, P.S., 1993. Estimation of continental precipitation recycling. J. Clim. 6, 1077–1089.

Brutsaert, W., Parlange, M.B., 1998. Hydrologic cycle explains the evaporation paradox. Nature 396, 29–30. https://doi.org/10.1038/23845.

Chen, Y., Takeuchi, K., Xu, C., Chen, Y., Xu, Z., 2006. Regional climate change and its effects on river runoff in the Tarim Basin. China. Hydrol. Proce. 20 (10), 2207–2216. https://doi.org/10.1002/hyp.6200.

Chen, Y., Li, W., Xu, C., Hao, X., 2007. Effects of climate change on water resources in Tarim River Basin, Northwest China. J. Environ. Sci. 19 (4), 488–493.

Chen, Y., Xu, C., Hao, X., Li, W., Chen, Y., Zhu, C., Ye, Z., 2009. Fifty-year climate change and its effect on annual runoff in the Tarim River Basin, China. Quat. Int. 208 (1), 53–61.

Chen, Y., Xu, C., Chen, Y., Liu, Y., Li, W., 2013a. Progress, challenges and prospects of ecohydrological studies in the Tarim River Basin of Xinjiang, China. Environ. Manag. 51 (1), 138–153. https://doi.org/10.1007/s00267-012-9823-8.

Chen, F., Chen, J., Huang, W., Chen, S., Huang, X., Jin, L., Feng, S., 2019a. Westerlies Asia and monsoonal Asia: Spatiotemporal differences in climate change and possible mechanisms on decadal to sub-orbital timescales. Earth Sci. Rev. 192, 337–354.

Chen, Z.S., Chen, Y.N., Li, B.F., 2013b. Quantifying the effects of climate variability and human activities on runoff for Kaidu River Basin in arid region of northwest China. Theor. Appl. Climatol. 111 (3–4), 537–545.

Chen, Y., Deng, H., Li, B., Li, Z., Xu, C., 2014. Abrupt change of temperature and precipitation extremes in the arid region of Northwest China. Quat. Int. 336, 35–43. https://doi.org/10.1016/j.quaint.2013.12.057.

Chen, Y.N., Li, B.F., Fan, Y.T., Sun, C.J., Fang, G.H., 2019b. Hydrological and water cycle processes of inland river basins in the arid region of Northwest China. J. Arid Land 11 (2), 161–179. https://doi.org/10.1007/s40333-019-0050-5.

Chen, Y., Li, Z., Fan, Y., Wang, H., Deng, H., 2015. Progress and prospects of climate change impacts on hydrology in the arid region of northwest China. Environ. Res. 139, 11–19. https://doi.org/10.1016/j.envres.2014.12.029.

Chen, Y., Li, W., Deng, H., Fang, G., Li, Z., 2016. Changes in Central Asia's Water Tower: Pastv. Scientific Rep. 6 (1), 35458. https://doi.org/10.1038/srep35458.

Chen, L.P., Li, Z.Q., Zhang, H., Huai, B.J., 2017. Temporal and spatial distribution of snow cover in Altai region, Xinjiang from 2001 to 2014. J. Arid Land Resour. Environ. 31 (3), 152–157 (In Chinese).

Chen, Y., et al., 2020. Potential risks and challenges of climate change in the arid region of northwestern China. Regional Sustain. https://doi.org/10.1016/j.regsus.2020.06.003.

Cheng, W.M., Zhou, C.H., Liu, H.J., Zhang, Y., Jiang, Y., Zhang, Y.C., Yao, Y.H., 2006. The oasis expansion and eco-environment change over the last 50 years in Manas River valley, Xinjiang. Sci. China Series D 49, 163–175.

China Meteorological Administration (CAM), 2019. Bule Book on Climate Change in China. China Science Press, Beijing.

Cong, Z.T., Yang, D.W., Ni, G.H., 2009. Does evaporation paradox exist in China? Hydrol. Earth Syst. Sci. 13, 357–366. https://doi.org/10.5194/hess-13-357-2009.

Dai, X., Li, W., Ma, Z., 2006. Variation characteristics of vapor sources in Xinjiang. Advance. Nature 16 (12), 1651–1656 (in Chinese). https://doi.org/10.3321/j.issn:1002-008X.2006.12.018.

Dai, X.G., Li, W.J., Ma, Z.G., Wang, P., 2007. Water-vapor source shift of Xinjiang region during the recent twenty years. Prog. Nat. Sci. 17, 569–575. https://doi.org/10.1080/10020070708541037.

Dansgaard, W., 1964. Stable isotopes in precipitation. Tellus 16 (4), 436–468. https://doi.org/10.3402/tellusa.v16i4.8993.

DeAngelis, A., Dominguez, F., Fan, Y., Robock, A., Kustu, M.D., Robinson, D., 2010. Evidence of enhanced precipitation due to irrigation over the Great Plains of the United States. J. Geophys. Res. 115, D15115.

Deng, H., Chen, Y., Shi, X., Li, W., Wang, H., Zhang, S., Fang, G., 2014. Dynamics of temperature and precipitation extremes and their spatial variation in the arid region of northwest China. Atmos. Res. 138 (138), 346–355.

Dittrich, A., Buerkert, A., Brinkmann, K., 2010. Assessment of land use and land cover changes during the last 50 years in oases and surrounding rangelands of Xinjiang, NW China. J. Agr. Rural Develop. Trop. Subtrop. 111, 129–142.

Dominguez, F., Kumar, P., Vivoni, E.R., 2008. Precipitation recycling variability and ecoclimatological stability — a study using NARR data. Part II: North American monsoon region. J. Clim. 21, 5187–5203. https://doi.org/10.1175/2008JCLI1760.1.

Donat, M.G., Lowry, A.L., Alexander, L.V., O' Gorman, P.A., Maher, N., 2016. More extreme precipitation in the world' s dry and wet regions Nat. Clim. Chang. 6, 508–513.

Dong, W., Cui, B.S., Liu, Z.H., et al., 2015. Relative effects of human activities and climate change on the river runoff in an arid basin in northwest China. Hydrol. Process. 28 (18), 4854–4864.

Doris, D., Christoph, M., Tong, J., Sergiy, V., 2016. Projections for headwater catchments of the Tarim River reveal glacier retreat and decreasing surface water availability but uncertainties are large. Environ. Res. Lett. 11 (5), 054024.

Draxler, R.R., Hess, G., 1998. An overview of the HYSPLIT_4 modelling system for trajectories. Aust. Meteorol. Mag. 47 (4), 295–308.

Drumond, A., Nieto, R., Gimeno, L., 2011. On the contribution of the Tropical Western hemisphere warm pool source of moisture to the Northern Hemisphere precipitation through a Lagrangian approach. J. Geophys. Res.-Atmos. 116 (D21) https://doi.org/10.1029/2010JD015397.

Fan, Y.T., Chen, Y.N., Li, X.G., Li, W.H., Li, Q.H., 2015. Characteristics of water isotopes and ice-snowmelt quantification in the Tizinafu River, north Kunlun Mountains, Central Asia. Quat. Int. 380, 116–122.

Fang, S.F., Yan, J., Che, M., Zhu, Y., Liu, Z., Pei, H., Lin, X., 2013. Climate change and the ecological responses in Xinjiang, China: model simulations and data analyses. Quat. Int. 311, 108–116.
Fang, G.H., Yang, J., Chen, Y.N., et al., 2018. How hydrologic processes differ spatially in a large basin: multisite and multiobjective modeling in the Tarim River Basin. J. Geophys. Res. Atmos. 123 (4), 7089–7113.
Farinotti, D., Longuevergne, L., Moholdt, G., Duethmann, D., Mölg, T., Bolch, T., Güntner, A., 2015. Substantial glacier mass loss in the Tien Shan over the past 50 years. Nat. Geosci. 8 (9), 716.
Farinotti, D., Immerzeel, W.W., de Kok, R.J., Quincey, D.J., Dehecq, A., 2020. Manifestations and mechanisms of the Karakoram glacier Anomaly. Nat. Geosci. 13 (1), 8-+.
Fu, B.P., 1981. On the calculation of evaporation from land surface. Sci. Atmos. Sin. 5, 23–31 [in Chinese].
Gao, X., Ye, B.S., Zhang, S.Q., et al., 2010. Glacier runoff variation and its influence on river runoff during 1961–2006 in the Tarim River Basin, China. Sci. China Ser. D Earth Sci. 40 (5), 654–665.
Gao, G., Xu, C.Y., Chen, D., Singh, V.P., 2012. Spatial and temporal characteristics of actual evapotranspiration over Haihe River basin in China. Stoch. Env. Res. Risk A. 26 (5), 655–669.
Gao, F., Zhang, Y., Chen, Q., Wang, P., Yang, H., Yao, Y., Cai, W., 2018. Comparison of two long-term and high-resolution satellite precipitation datasets in Xinjiang, China. Atmos. Res. 212, 150–157.
Gao, L., Deng, H., Lei, X., Wei, J., Chen, Y., Li, Z., Ma, M., Chen, X., Chen, Y., Liu, M., Gao, J., 2020. Evidence for elevation-dependent warming from the Chinese Tianshan Mountains. Cryosphere Discuss. https://doi.org/10.5194/tc-2020-188 in review.
Gimeno, L., 2013. Grand challenges in atmospheric science. Front. Earth Sci. 1, 1–5. https://doi.org/10.3389/feart.2013.00001.
Gimeno, L., Vázquez, M., Eiras-Barca, J., et al., 2019. Recent progress on the sources of continental precipitation as revealed by moisture transport analysis. Earth Sci. Rev. https://doi.org/10.1016/j.earscirev.2019.103070.
Guan, X., Yang, L., Zhang, Y., Li, J., 2019. Spatial distribution, temporal variation, and transport characteristics of atmospheric water vapor over Central Asia and the arid region of China. Glob. Planet. Chang. 172, 159–178. https://doi.org/10.1016/j.gloplacha.2018.06.007.
Guan, J.Y., Yao, J.Q., Li, M.Y., Li, D., Zheng, J.H., 2021. Historical changes and projected trends of extreme climate events in Xinjiang. Climatic Dynamic, accepted, China.
Guo, L., Li, L., 2015. Variation of the proportion of precipitation occurring as snow in the Tian Shan Mountains, China. Int. J. Climatol. 35 (7), 1379–1393.
Guo, Y., Shen, Y., 2016. Agricultural water supply/demand changes under projected future climate change in the arid region of northwestern China. J. Hydrol. 540, 257–273. https://doi.org/10.1016/j.jhydrol.2016.06.033.
Guo, M., Wu, W., Zhou, X., Chen, Y., Li, J., 2015. Investigation of the dramatic changes in lake level of the Bosten Lake in northwestern China. Theor. Appl. Climatol. 119 (1-2), 341–351.
Guo, J., Huang, G., Wang, X., Li, Y., Lin, Q., 2017. Investigating future precipitation changes over China through a high-resolution regional climate model ensemble. Earth's Future 5 (3), 285–303. https://doi.org/10.1002/2016EF000433.
Hao, J., Huang, F., Liu, Y., Amobichukwu, C.A., Li, L., 2018. Avalanche activity and characteristics of its triggering factors in the western Tianshan Mountains, China. J. Mt. Sci. 15 (7), 1397–1411.
Hewitt, K., 2005. The Karakoram anomaly? Glacier expansion and the 'Elevation Effect,' Karakoram Himalaya. Mount. Res. Dev. 25, 332–340.
Hu, Y.N., Duan, W.L., Chen, Y.N., et al., 2021. An integrated assessment of runoff dynamics in the Amu Darya River Basin: confronting climate change and multiple human activities, 1960 – 2017. J. Hydrol. 603, 126905.
Hua, L., Zhong, L., Ma, Z., 2017. Decadal transition of moisture sources and transport in Northwestern China during summer from 1982 to 2010. J. Geophys. Res.-Atmos. 122 (23), 12522–12540. https://doi.org/10.1002/2017 JD027728.
Huai, B., Li, Z., Sun, M., Wang, W., Jin, S., Li, K., 2015. Change in glacier area and thickness in the Tomur Peak, western Chinese Tien Shan over the past four decades. J. Earth Syst. Sci. 124 (2), 353–363. https://doi.org/10.1007/s12040-015-0541-5.
Huai, B., Sun, W., Wang, Y., Li, Z., 2017. Glacier Shrinkage in the Chinese Tien Shan Mountains from 1959/1972 to 2010/2012. Arct. Antarct. Alp. Res. 49 (2), 213–225. https://doi.org/10.1657/AAAR0015-032.
Huang, W., Chen, F.H., Feng, S., Chen, J.H., Zhang, X.J., 2013. Interannual precipitation variations in the midlatitude Asia and their association with large scale atmospheric circulation. Chin. Sci. Bull. 58, 3963–3968.
Huang, W., Feng, S., Chen, J.-H., et al., 2015. Physical mechanisms of summer precipitation variations in the Tarim Basin in northwestern China. J. Clim. 28 (9), 3579–3591.
Huang, J.P., Ji, M.X., Xie, Y.K., Wang, S.S., He, Y.L., Ran, J.T., 2016a. Global semi-arid climate change over last 60 years. Clim. Dyn. 46 (3–4), 1131–1150. https://doi.org/10.1007/s00382-015-2636-8.
Huang, J.P., Yu, H.P., Guan, X.D., Wang, G.Y., Guo, R.X., 2016b. Accelerated dryland expansion under climate change. Nat. Clim. Chang. 6 (2), 166–171. https://doi.org/10.1038/nclimate2837.
Huang, W., Chang, S., Xie, C., Zhang, Z., 2017b. Moisture sources of extreme summer precipitation events in North Xinjiang and their relationship with atmospheric circulation. Adv. Clim. Chang. Res. 8 (1), 12–17. https://doi.org/10.1016/j.accre.2017.02.001.
IPCC, Stocker, T.F., 2013. Summary for Policymakers. In: Qin, D., Plattner, G.-K., Tignor, M., Allen, S.K., Boschung, J., Nauels, A., Xia, Y., Bex, V., Midgley, P.M. (Eds.), Climate Change 2013: The Physical Science Basis. Contribution of Working Group I to the Fifth Assessment Report of the Intergovernmental Panel on Climate Change. Cambridge University Press, Cambridge, United Kingdom and New York, NY, USA.
Jiang, Y., Chen, Y., Zhao, Y., Chen, P., Yu, X., Fan, J., Bai, S., 2013. Analysis on changes of basic climatic elements and extreme events in xinjiang, China during 1961–2010. Adv. Clim. Chang. Res. 4 (1), 20–29. https://doi.org/10.3724/SP.J.1248.2013.020.
Jiang, Z., Jiang, S., Shi, Y., Liu, Z., Li, W., Li, L., 2017. Impact of moisture source variation on decadal-scale changes of precipitation in North China from 1951 to 2010. J. Geophys. Res. Atmos. 122, 600–613.
Josef, C., Hung, L.Y., Li, Z.L., 1997. Multi-temporal, multi-channel AVHRR data sets for land biosphere studies-artifacts and corrections. Remote Sens. Environ. 60, 35–57. https://doi.org/10.1016/S0034-4257(96)00137-X.
Kääb, A., Berthier, E., Nuth, C., Gardelle, J., Arnaud, Y., 2012. Contrasting patterns of early twenty-first-century glacier mass change in the Himalayas. Nature 488, 495–498.
Kang, S., You, Q., Fl, W., Pepin, N., Yao, T., 2010. Review of climate and cryospheric change in the Tibetan Plateau. Environ. Res. Lett. 5 (1), 015101 https://doi.org/10.1088/1748-9326/5/1/015101.
Karl, T.R., Arguez, A., Huang, B., Lawrimore, J.H., Mcmahon, J., Menne, M.J., Zhang, H., 2015. Possible artifacts of data biases in the recent global surface warming hiatus. Science 348 (6242), 1469–1472.
Kong, Y., Pang, Z., 2012. Evaluating the sensitivity of glacier rivers to climate change based on hydrograph separation of discharge. J. Hydrol. 434–435, 121–129. https://doi.org/10.1016/j.jhydrol.2012.02.029.
Kosaka, Y., Xie, S., 2013. Recent global-warming hiatus tied to equatorial Pacific surface cooling. Nature 501 (7467), 403–407.
Li, Y., Morrill, C., 2013. Lake levels in Asia at the Last Glacial Maximum as indicators of hydrologic sensitivity to greenhouse gas concentrations. Quat. Sci. Rev. 60, 1–12.
Li, Z.X., Feng, Q., Li, Z.J., Yuan, R.F., Gui, J., Lv, Y.M., 2019. Climate background, fact and hydrological effect of multiphase water transformation in cold regions of the Western China: A review. Earth Sci. Rev. 190, 33–57. https://doi.org/10.1016/j.earscirev.2018.12.004.
Li, Z.Q., Li, H.L., Chen, Y.N., 2011. Mechanisms and simulation of accelerated shrinkage of continental glaciers: a case study of Urumqi Glacier No. 1 in eastern Tianshan, Central Asia. J. Earth Sci. 22 (4), 423–430.
Li, Q., Chen, Y., Shen, Y., Li, X., Xu, J., 2011b. Spatial and temporal trends of climate change in Xinjiang, China. J. Geogr. Sci. 21 (6), 1007–1018.
Li, B., Chen, Y., Shi, X., 2012. Why does the temperature rise faster in the arid region of northwest China? J. Geophys. Res.-Atmos. 117 (D16) https://doi.org/10.1029/2012JD017953.
Li, D., Pan, M., Cong, Z., Zhang, L., Wood, E., 2013a. Vegetation control on water and energy balance within the Budyko framework. Water Resour. Res. 49, 1–8. https://doi.org/10.1002/wrcr.20107.
Li, Z., Chen, Y.N., Shen, Y.J., et al., 2013b. Analysis of changing pan evaporation in the arid region of Northwest China. Water Resour. Res. 49, 2205–2212. https://doi.org/10.1002/wrcr.20202.
Li, B.F., Chen, Y.N., Xiong, H.G., 2016a. Quantitatively evaluating the effects of climate factors on runoff change for Aksu River in northwestern China. Theor. Appl. Climatol. 123 (1–2), 97–105.
Li, X.P., Wang, L., Guo, X., Chen, D., 2017a. Does summer precipitation trend over and around the Tibetan Plateau depend on elevation? Int. J. Climatol. 37 (Suppl), 1278–1284. https://doi.org/10.1002/joc.4978.
Li, Z., Chen, Y.N., Fang, G.H., Li, Y.P., 2017b. Multivariate assessment and attribution of droughts in CentralAsia. Sci. Rep-UK. 7, 1316.
Li, X.F., Yao, X.J., Sun, M.P., et al., 2018. Spatial-temporal variations in lakes in northwest China from 2000 to 2014. Acta Ecol. Sin. 38 (1), 96–104. https://doi.org/10.5846/stxb201612262677.
Li, Z., Chen, Y., Li, Y., Wang, Y., 2020a. Declining snowfall fraction in the alpine regions, Central Asia. Sci. Rep. 10 (1), 3476. https://doi.org/10.1038/s41598-020-60303-z.
Li, J., Liu, G., Kwak, J.H., et al., 2020b. Reclamation of desert land to continuous cotton cropping affects soil properties and microbial communities in the desert-oasis ecotone of Xinjiang, China. J. Soils Sediments 20, 862–873. https://doi.org/10.1007/s11368-019-02469-2.
Li, M., Yao, J., Guan, J., 2021. Observed changes in vapor pressure deficit suggest a systematic drying of the atmosphere in Xinjiang of China. Atmos. Res. 248, 105199 https://doi.org/10.1016/j.atmosres.2020.105199.
Ling, H.B., Xu, H.L., Zhang, Q.Q., 2012. Nonlinear analysis of runoff changes and climate factors in the headstream of Keriya River, Xinjiang. Geogr. Res. 31, 792–802.
Liu, S.Y., Yao, X.J., Guo, W.Q., Xu, J.L., Shangguan, D.H., Wei, J.F., et al., 2015. The contemporary glaciers in China based on the second Chinese glacier inventory. Acta Geograph. Sin. 70 (1), 3–16 (In Chinese).
Liu, H., Chen, Y., Ye, Z., Li, Y., Zhang, Q., 2019. Recent lake area changes in Central Asia. Sci. Rep. 9, 16277. https://doi.org/10.1038/s41598-019-52396-y.
Liu, J., Liu, F., Tuoliewubieke, D., Yang, L., 2020. Analysis of the water vapour transport and accumulation mechanism during the "7.31" extreme rainstorm event in the southeastern Hami area, China. Meteorol. Appl. 27, e1933 https://doi.org/10.1002/met.1933.
Lo, M., Famiglietti, J.S., 2013. Irrigation in California's Central Valley strengthens the southwestern U.S. water cycle. Geophys. Res. Lett. 40, 301–306.
Lu, B., Li, H., Wu, J., et al., 2019. Impact of El Niño and Southern Oscillation on the summer precipitation over Northwest China. Atmos. Sci. Lett. 20, e928 https://doi.org/10.1002/asl.928.
Ma, Z.G., Fu, C.B., Yang, Q., Zheng, Z.Y., Lv, M.X., Duan, Y.W., Chen, L., 2018. Drying trend in northern China and its shift during 1951–2016. Chinese J. Atmos. Sci. (in Chinese) 42 (4), 951–961. https://doi.org/10.3878/j.issn.1006-9895.1802.18110.
Ma, M., Wang, X., Veroustraete, F., Dong, L., 2007. Change in area of Ebinur Lake during the 1998–2005 period. Int. J. Remote Sens. 28, 5523–5533.

Mason, I.M., Guzkowska, M.A.J., Rapley, C.G., 1994. The response of lake levels and areas to climatic change. Clim. Chang. 27, 161–197.
Neilson, R.P., 1993. The transient ecotone response to climatic change: some conceptual and modelling approaches. Ecol. Appl. 3, 385–395.
Pepin, N., Bradley, R.S., Diaz, H.F., Baraer, M., Caceres, E.B., Forsythe, N., Yang, D.Q., 2015. Elevation-dependent warming in mountain regions of the world. Nat. Clim. Chang. 5 (5), 424–430. https://doi.org/10.1038/nclimate2563.
Pi, H., Sharratt, B.S., Lei, J., 2017. Windblown sediment transport and loss in a desert–oasis ecotone in the Tarim Basin. Sci. Rep. 7, 7723. https://doi.org/10.1038/s41598-017-04971-4.
Piao, S., Ciais, P., Huang, Y., Shen, Z., Peng, S., Li, J., Zhou, L., Liu, H., Ma, Y., Ding, Y., 2010. The impacts of climate change on water resources and agriculture in China. Nature 467 (7311), 43–51.
Qin, D.H., Ding, Y.H., Su, J.L., Ren, J.W., Wang, S.W., Wu, R.S., Yang, X.Q., Wang, S.M., Liu, S.Y., Dong, G.R., Lu, Q., Huang, Z.G., Du, B.L., Luo, Y., 2005. Assessment of climate and environment evolution in China (I): Climate and environmental changes and future trends in China. Adv. Clim. Chang. Res. 4–9. In Chinese.
Qin, J., Liu, Y., Chang, Y., Liu, S., Pu, H., Zhou, J., 2016. Regional runoff variation and its response to climate change and human activities in Northwest China. Environ. Earth Sci. 75 (20), 1–14. https://doi.org/10.1007/s12665-016-6187-z.
Roderick, M.L., Farquhar, G.D., 2002. The cause of decreased pan evaporation over the past 50 years. Science 298, 1410–1411. https://doi.org/10.1126/science.1075390-a.
Roderick, M.L., Rotstayn, L.D., Farquhar, G.D., et al., 2007. On the attribution of changing pan evaporation. Geophys. Res. Lett. 34, L17403. https://doi.org/10.1029/2007GL031166.
Roe, G.H., Baker, M.B., Herla, F., 2017. Centennial glacier retreat as categorical evidence of regional climate change. Nat. Geosci. 10 (2), 95.
Schär, C., Lüthi, D., Beyerle, U., et al., 1999. The soil-precipitation feedback: a process study with a regional climate model. J. Clim. 12 (3), 722–741.
Serquet, G., Marty, C., Dulex, J.P., Rebetez, M., 2011. Seasonal trends and temperature dependence of the snow-fall/precipitation-day ratio in Switzerland. Geophys. Res. Lett. 38 (7), L07703.
Shangguan, D., Liu, S., Ding, Y., Ding, L., Xu, J., Li, J., 2009. Glacier changes during the last forty years in the tarim interior river basin, Northwest China. Prog. Nat. Sci.: Mater. Int. 19 (6), 727–732.
Shen, Y.-J., Shen, Y., Fink, M., Kralisch, S., Brenning, A., 2018. Unraveling the hydrology of the glacierized kaidu basin by integrating multisource data in the Tianshan Mountains, Northwestern China. Water Resour. Res. 54 (1), 557–580.
Shen, Y., Guo, Y., Zhang, Y., Pei, H., Brenning, A., 2020. Review of historical and projected future climatic and hydrological changes in mountainous semiarid Xinjiang (northwestern China), central Asia. Catena 187, 104343. https://doi.org/10.1016/j.catena.2019.104343.
Shi, Y., Shen, Y., Li, D., et al., 2003. Discussion on the present climate change from warm-dry to warm-wet in Northwest China. Quat. Sci. 23 (2), 152–164. https://doi.org/10.3321/j.issn:1001-7410.2003.02.005 (in Chinese).
Shi, Y., Shen, Y., Kang, E., Li, D., Ding, Y., Zhang, G., Hu, R., 2007. Recent and future climate change in northwest China. Clim. Chang. 80 (3–4), 379–393.
Sorg, A., Bolch, T., Stoffel, M., Solomina, O., Beniston, M., 2012. Climate change impacts on glaciers and runoff in Tien Shan (Central Asia). Nat. Clim. Chang. 2 (10), 725.
Stidd, C.K., 1975. Irrigation increases rainfall? Science 188, 279–281.
Stohl, A., James, P., 2005. A Lagrangian analysis of the atmospheric branch of the global water cycle. Part II: Moisture transports between Earth's ocean basins and river catchments. J. Hydrometeorol. 6, 961–984. https://doi.org/10.1175/JHM470.1.
Stohl, A., Forster, F., Sodemann, H., 2008. Remote source of water vapor forming precipitation on the Norwegian west coast at 60 N —A tale of hurricanes and an atmospheric river. J. Geophys. Res. 113, D05102. https://doi.org/10.1029/2007JD009006.
Sun, M.P., Li, Z.Q., Yao, X.J., et al., 2013. Rapid shrinkage and hydrological response of a typical continental glacier in the arid region of northwest China: Taking Urumqi Glacier No. 1 as an example. Ecohydrology 6 (6), 909–916.
Sun, C.J., Chen, Y.N., Li, X.G., et al., 2016a. Analysis on the streamflow components of the typical inland river, Northwest China. Hydrol. Sci. J. 61 (5), 970–981.
Sun, C.J., Chen, Y.N., Li, W.H., et al., 2016b. Isotopic time series partitioning of streamflow components under regional climate change in the Urumqi River, northwest China. Hydrol. Sci. J. 61 (8), 1443–1459.
Tang, X.L., Lv, X., Li, J.F., 2011. Runoff characteristics of Manasi River Basin in the past 50 years. J Arid Land Resour Environ 25, 124–129.
Van der Ent, R.J., Savenije, H.H.G., 2011. Length and time scales of atmospheric moisture recycling. Atmos. Chem. Phys. 11 (5), 1853–1863. https://doi.org/10.5194/acp-11-1853-2011.
Vicente-Serrano, S.M., Beguería, S., López-Moreno, J.I., 2010. A multiscalar drought index sensitive to global warming: the standardized precipitation evapotranspiration index. J. Clim. 23 (7), 1696–1718. https://doi.org/10.1175/2009JCLI2909.1.
Wang, Q., Zhai, P.M., Qing, D.H., 2020. New perspectives on 'warming–wetting' trend in Xinjiang, China. Adv. Clim. Chang. Res. 11 (3), 252–260.
Wang, L., Chen, W., 2014. A CMIP5 multimodel projection of future temperature, precipitation, and climatological drought in China. Int. J. Climatol. 34 (6), 2059–2078. https://doi.org/10.1002/joc.3822.
Wang, X.R., Xu, X.D., Wang, W.G., 2007a. Characteristic of spatial transportation of water vapor for Northwest China's rainfall in spring and summer (in Chinese). Plateau Meteor. 26, 749–758.
Wang, H., Wang, S.L., Yu, X.J., Wang, M.X., Han, X.Y., 2020c. Spatial-temporal variation of snow cover in Xinjiang based on surface observation from 1961 to 2017. J. Glaciol. Geocryol. 42 (1), 72–80.
Wang, Y., Xiao, D., Li, Y., 2007b. Temporal–spatial change in soil degradation and its relationship with landscape types in a desert–oasis ecotone: a case study in the Fubei region of Xinjiang Province, China. Environ. Geol. 51, 1019–1028.
Wang, B., Bao, Q., Hoskins, B.J., Wu, G., Liu, Y., 2008. Tibetan Plateau warming and precipitation changes in East Asia. Geophys. Res. Lett. 35 (14) https://doi.org/10.1029/2008GL034330.
Wang, H., Chen, Y., Li, W., Deng, H., 2013a. Runoff responses to climate change in arid region of northwestern China during 1960–2010. Chin. Geogr. Sci. 23 (3), 286–300. https://doi.org/10.1007/s11769-013-0605-x.
Wang, Y.F., Shen, Y.J., Chen, Y.N., et al., 2013b. Vegetation dynamics and their response to hydroclimatic factors in the Tarim River Basin, China. Ecohydrology 6, 927–936. https://doi.org/10.1002/eco.1255.
Wang, X., Li, Z., Tayier, R.E., Ruo, Z., Zhou, P., 2015. Characteristics of water isotopes and hydrograph separation during the spring flood period in Yushugou River basin, Eastern Tianshans, China. J. Earth Syst. Sci. 124 (1), 115–124.
Wang, S., Zhang, M., Che, Y., Chen, F., Qiang, F., 2016. Contribution of recycled moisture to precipitation in oases of arid central Asia: A stable isotope approach. Water Resour. Res. 52 (4), 3246–3257.
Wang, Y., Zhou, B., Qin, D., Wu, J., Gao, R., Song, L., 2017. Changes in mean and extreme temperature and precipitation over the arid region of Northwestern China: observation and projection. Adv. Atmos. Sci. 34 (3), 289–305.
Wang, N., Yao, T., Xu, B., Chen, A.a. and Wang, W., 2019. Spatiotemporal Pattern, Trend, and Influence of Glacier Change in Tibetan Plateau and Surroundings under Global Warming. Bull. Chin. Acad. Sci. 34 (11), 1220–1232.
Wang, B., Ma, Y., Su, Z., Wang, Y., Ma, W., 2020a. Quantifying the evaporation amounts of 75 high-elevation large dimictic lakes on the Tibetan Plateau. Sci. Adv. 6, eaay8558. https://doi.org/10.1126/sciadv.aay8558.
Wang, Z.Q., Gao, X.J., Tong, Y., 2021. Future climate change projection over Xinjiang based on an ensemble of regional climate model simulations. Chinese J. Atmos. Sci. (in Chinese) 45 (2), 407–423. https://doi.org/10.3878/j.issn.1006-9895.2006.20108.
Wang, G., Gou, Q., Hao, Y., Zhao, H., Zhang, X., 2020b. Dynamics of soil water content across different landscapes in a typical desert-oasis ecotone. Front. Environ. Sci. 8, 577406 https://doi.org/10.3389/fenvs.2020.577406.
Wu, Z., Zhang, H., Krause, C.M., Cobb, N.S., 2010. Climate change and human activities: a case study in Xinjiang, China. Clim. Chang. 99 (3), 457–472. https://doi.org/10.1007/s10584-009-9760-6.
Wu, P., Ding, Y., Liu, Y., Li, X., 2019. The characteristics of moisture recycling and its impact on regional precipitation against the background of climate warming over Northwest China. Int. J. Climatol. 39, 5241–5255. https://doi.org/10.1002/joc.6136.
Xu, C., Chen, Y., Yang, Y., Hao, X., Shen, Y., 2010. Hydrology and water resources variation and its response to regional climate change in Xinjiang. J. Geogr. Sci. 20 (4), 599–612.
Xu, C., Li, J., Zhao, J., Gao, S., Chen, Y., 2015. Climate variations in northern Xinjiang of China over the past 50 years under global warming. Quat. Int. 358, 83–92. https://doi.org/10.1016/j.quaint.2014.10.025.
Xu, C., Zhao, J., Deng, H., Fang, G., Tan, J., He, D., Chen, Y., Chen, Y., Fu, A., 2016. Scenario-based runoff prediction for the Kaidu River basin of the Tianshan Mountains, Northwest China. Environ. Earth Sci. 75 (15), 1126. https://doi.org/10.1007/s12665-016-5930-9.
Xue, J., Gui, D.W., Zhao, Y., Lei, J.Q., Feng, X.L., Zeng, F.J., Mao, D.L., 2015. Quantification of environmental flow requirements to support ecosystem services of Oasis Areas: a case study in Tarim Basin, Northwest China. Water 7, 5657–5675.
Xue, J., Gui, D.W., Lei, J.Q., 2019. Oasification: an unable evasive process in fighting against desertification for the sustainable development of arid and semiarid regions of China. Catena 179, 197–209. https://doi.org/10.1016/j.catena.2019.03.029.
Yang, H.B., Yang, D.W., 2011. Climatic factors influencing changing pan evaporation across China from 1961 to 2001. J. Hydrol. 414–415, 184–193. https://doi.org/10.1016/j.jhydrol.2011.10.043.
Yang, L.M., Zhang, Q.Y., 2007. Circulation characteristics of interannual and Interdecandal anomalies of summer rainfall in north Xinjiang (in Chinese). Chin. J. Geophys. 50, 412–419.
Yang, L.M., Guang, X.F., Zhang, Y.X., 2018. Study on atmospheric circulation characteristics of precipitation anomalies in arid region of Central Asia. Arid Zone Research 35 (02), 249–259.
Yang, D., Sun, F., Liu, Z., Cong, Z., Lei, Z., 2006. Interpreting the complementary relationship in nonhumid environments based on the Budyko and Penman hypotheses. Geophys. Res. Lett. 33, L18402. https://doi.org/10.1029/2006GL027657.
Yang, Y.H., Fang, J.Y., Ma, W.H., Smith, P., Mohammat, A., Wang, S.P., Wang, W., 2010. Soil carbon stock and its changes in northern China's grasslands from 1980s to 2000s. Glob. Chang. Biol. 16, 3036–3047.
Yang, L.M., Zhang, Y.H., Tang, H., 2012. Analyses on water vapor characteristic in three heavy rainstorm processes of Xinjiang in July 2007 (in Chinese). Plateau Meteor. 31, 963–973.
Yao, J.Q., Zhao, Q.D., Liu, Z.H., et al., 2015. Effect of climate variability and human activities on runoff in the Jinghe River Basin, Northwest China. J. Mt. Sci. 12 (2), 358–367. https://doi.org/10.1007/S11629-014-3081-7.
Yao, J.Q., Yang, Q., Mao, W.Y., Zhao, Y., Xu, X.B., 2016a. Precipitation trend–Elevation relationship in arid regions of the China. Glob. Planet. Chang. 143, 1–9.
Yao, J.Q., Yang, Q., Wu, L.K., Xu, Xi.B., 2016b. Quantifying recycled moisture fraction in precipitation of Tianshan mountains. Desert Oasis Meteorol. 10 (5), 37–43 (In Chinese).

Yao, J., Mao, W., Yang, Q., Xu, X., Liu, Z., 2017. Annual actual evapotranspiration in inland river catchments of China based on the Budyko framework. Stoch. Env. Res. Risk A. 31 (6), 1409–1421.
Yao, J., Zhao, Y., Chen, Y., Yu, X., Zhang, R., 2018a. Multi-scale assessments of droughts: A case study in Xinjiang, China. Sci. Total Environ. 630, 444–452.
Yao, J.Q., Chen, Y.N., Zhao, Y., Mao, W., Xu, X., Liu, Y., Yang, Q., 2018b. Response of vegetation NDVI to climatic extremes in the arid region of Central Asia: a case study in Xinjiang, China. Theoretical Appl. Climatol. 131 (3–4), 1503–1515. https://doi.org/10.1007/s00704-017-2058-0.
Yao, S.B., Jiang, D.B., Zhang, Z.S., 2020d. Lagrangian simulations of moisture sources for Chinese Xinjiang precipitation during 1979–2018. Int. J. Climatol. https://doi.org/10.1002/joc.6679.
Yao, J., Li, M., Yang, Q., 2018c. Moisture sources of a torrential rainfall event in the arid region of East Xinjiang, China, based on a Lagrangian model. Nat. Hazards 92 (1), 183–195.
Yao, J., Chen, Y., Zhao, Y., Yu, X., 2018d. Hydroclimatic changes of Lake Bosten in Northwest China during the last decades. Sci. Rep. 8, 9118. https://doi.org/10.1038/s41598-018-27466-2.
Yao, T., Xue, Y., Chen, D., Chen, F., Thompson, L.G., Cui, P., Li, Q., 2019a. Recent third pole's rapid warming accompanies cryospheric melt and water cycle intensification and interactions between monsoon and environment: multidisciplinary approach with observations, modeling, and analysis. Bull. Am. Meteorol. Soc. 100 (3), 423–444. https://doi.org/10.1175/BAMS-D-17-0057.1.
Yao, J., Hu, W., Chen, Y., et al., 2019b. Hydro-climatic changes and their impacts on vegetation in Xinjiang, Central Asia. Sci. Total Environ. 660, 724–732.
Yao, J.Q., Chen, Y.N., Zhao, Y., 2020a. Study on Atmospheric Water Cycle Process and Its Influence in Northwest Arid Region of China. China Meteorological Press, Beijing.
Yao, J., Chen, Y., Zhao, Y., Guan, X., Mao, W., Yang, L., 2020b. Climatic and associated atmospheric water cycle changes over the Xinjiang, China. J. Hydrol. 585, 124823 https://doi.org/10.1016/j.jhydrol.2020.124823.
Yao, J., Chen, Y., Yu, X., Zhao, Y., Guan, X., Yang, L., 2020c. Evaluation of multiple gridded precipitation datasets for the arid region of northwestern China. Atmos. Res. 236, 104818 https://doi.org/10.1016/j.atmosres.2019.104818.
Yao, J.Q., Chen, Y.N., Chen, J., Zhao, Y., Dilinuer, T., Li, J.G., Yang, L.M., Mao, W.Y., 2021. Intensification of extreme precipitation in arid Central Asia. J. Hydrol 598, 125760. https://doi.org/10.1016/j.jhydrol.2020.125760.
Yatagai, A., 2003. Evaluation of hydrological balance and its variability in arid and semi-arid regions of Eurasia from ECMWF 15-year reanalysis. Hydrol. Process. 17, 2871–2884. https://doi.org/10.1002/hyp.1439.
Ye, W., Wang, F., Li, Z., Zhang, H., Xu, C., Huai, B., 2016. Temporal and spatial distributions of the equilibrium line altitudes of the monitoring glaciers in High Asia. J. Glaciol. Geocryol. 38 (6), 1459–1469.
You, Q.L., Wu, T., Shen, L.C., Pepin, N., Zhang, L., Jiang, Z.H., Wu, Z.W., Kang, S.C., AghaKouchak, A., 2020. Review of snow cover variation over the Tibetan Plateau and its influence on the broad climate system. Earth Sci. Rev. 201, 103043 https://doi.org/10.1016/j.earscirev.2019.103043.
Yu, Y., Chen, X., Disse, M., Cyffka, B., Lei, J., Zhang, H., Yu, R., 2020. Climate change in Central Asia: Sino-German cooperative research findings. Sci. Bull. 65, 689. https://doi.org/10.1016/j.scib.2020.02.008.
Yue, X., Liu, G., Chen, J., Zhou, C., 2020. Synergistic regulation of the interdecadal variability in summer precipitation over the Tianshan mountains by sea surface temperature anomalies in the high-latitude Northwest Atlantic Ocean and the Mediterranean Sea. Atmos. Res. 233, 104717. https://doi.org/10.1016/j.atmosres.2019.104717.
Zhang, Q., Xu, C.-Y., Tao, H., Jiang, T., Chen, Y., 2010. Climate changes and their impacts on water resources in the arid regions: a case study of the Tarim River basin, China. Stoch. Env. Res. Risk A. 24 (3), 349–358. https://doi.org/10.1007/s00477-009-0324-0.
Zhang, X., Alexander, L., Hegerl, G.C., Jones, P., Tank, A.K., Peterson, T.C., Zwiers, F.W., 2011. Indices for monitoring changes in extremes based on daily temperature and precipitation data. Wiley Interdiscip. Rev. Clim. Chang. 2 (6), 851–870.
Zhang, D.H., Li, X.F., Yao, X.J., 2018b. A dataset of main lakes in northwest China with an area above 10 km^2 (2000-2014). Science Data Bank 3 (4). https://doi.org/10.11922/sciencedb.621.
Zhang, L., Lu, H.Q., Wang, L.Y., Yang, B.H., 2016. Spatial-temporal characteristics of soil moisture in China. Acta Geograph. Sin. 71 (9), 1494–1508.
Zhang, Q., Shi, P.J., Singh, V.P., Fan, K.K., Huang, J.J., 2017d. Spatial downscaling of TRMM-based precipitation data using vegetative response in Xinjiang, China. Int. J. Climatol. 37 (10), 3895–3909.
Zhang, T.X., Wang, H., Zhang, L.C., 2021. Assessment Report on Regional Climate Change in XJ: 2020. China Meteorology Press, Beijing.
Zhang, Y., Wei, W., Jiang, F., Liu, M., Wang, W., Bai, L., Li, K., 2012. Brief communication"Assessment of change in temperature and precipitation over Xinjiang, China". Nat.Hazards Earth Syst. Sci. 12, 1327–1331. https://doi.org/10.5194/nhess-12-1327-2012.
Zhang, G., Yao, T., Shum, C.K., Yi, S., Yang, K., Xie, H., et al., 2017a. Lake volume and groundwater storage variations in Tibetan Plateau's endorheic basin. Geophys. Res. Lett. 44 (11), 5550–5560.
Zhang, K., An, Z., Cai, D., Guo, Z., Xiao, J., 2017b. Key role of desert-oasis transitional area in avoiding oasis land degradation from Aeolian desertification in Dunhuang, Northwest China. Land Degrad. Dev. 28 (1), 142–150.
Zhang, Y., Fu, L., Pan, J., Xu, Y., 2017c. Projected changes in temperature extremes in china using PRECIS. Atmosphere 8 (1). https://doi.org/10.3390/atmos8010015.
Zhang, G.Q., Yao, T.D., Xie, H.J., Yang, K., Zhu, L.P., Shum, C.K., Bolch, T., Yi, S., Allen, S., Jiang, L.G., Chen, W.F., Ke, C.Q., 2020. Response of Tibetan Plateau lakes to climate change: trends, patterns, and mechanisms. Earth Sci. Rev. 208, 103269 https://doi.org/10.1016/j.earscirev.2020.103269.
Zhang, Y.H., Yu, B.X., Wang, Z.K., Jia, L.H., 2018a. Dynamic mechanism and water vapor transportation characteristics of two extreme rainstorm events in Ili River valley in summer of 2016 (in Chinese). Torrential Rain Disasters 37, 435–444.
Zhao, B.K., Cai, C.X., Yang, L.M., 2006. Atmospheric circulation anomalies during wetting summer over Xinjiang region. J. Glaciol. Geocryol. 28 (3), 434–442.
Zhao, Y., Huang, A., Zhou, Y., Huang, D., Yang, Q., Ma, Y., Li, M., Wei, G., 2014. Impact of the middle and upper tropospheric cooling over Central Asia on the summer rainfall in the Tarim Basin, China. J. Clim. 27 (12), 4721–4732.
Zhao, Y., Yu, X., Yao, J., Dong, X., Li, H., 2019. The concurrent effects of the South Asian monsoon and the plateau monsoon over the Tibetan Plateau on summer rainfall in the Tarim Basin of China. Int. J. Climatol. 39 (1), 74–88.
Zhao, Y., Zhang, H.Q., 2016. Impacts of SST warming in tropical Indian Ocean on CMIP5 model-projected summer rainfall changes over Central Asia. Clim. Dyn. 46 (9–10), 3223–3238.
Zhou, B., Wen, Q.H., Xu, Y., Song, L., Zhang, X., 2014. Projected changes in temperature and precipitation extremes in China by the CMIP5 multimodel ensembles. J. Clim. 27 (17), 6591–6611.
Zhou, Y., Xie, Z., Liu, X., 2019. An analysis of moisture sources of torrential rainfall events over Xinjiang, China. J. Hydrometeorol. 20 (10), 2109–2122.
Zhu, M., Yao, T., Yang, W., Xu, B., Wu, G., Wang, X., Xie, Y., 2018. Reconstruction of the mass balance of Muztag Ata No. 15 glacier, eastern Pamir, and its climatic drivers. J. Glaciol. 64 (244), 259–274.